

- I. [Abstract](#)
- II. [Introduction](#)
- III. [Simulation Modelling – using MODE](#)
- IV. [Layout Circuit Simulation – using Lumerical and Klayout](#)
- V. [Corner Analysis – using MODE](#)
- VI. [Corner Analysis Monte Carlo](#)
- VII. [Measurement Data](#)
- VIII. [Data Analysis using MATLAB](#)
- IX. [Conclusion](#)

Acknowledgements

Design Proposal : Mach-Zehnder Interferometer

Archana S (archana.arch03)

GDS File name : EBeam_archanas_v2.gds

I. Abstract

This report outlines details about the design of Mach-Zehnder Interferometer using Strip waveguide. The report presents simulated results and analytical expressions to corroborate the design choices. This design uses MZI using different components such as bidirectional coupler, directional coupler and adiabatic splitters in TE mode 1550nm. Simulation results shows difference in each of the approaches used and FSR is calculated for different in waveguide lengths.

II. Introduction

The Mach-Zehnder interferometer is a simple highly configurable device used to demonstrate interference by division of amplitude. The Mach-Zehnder interferometer can determine the relative phase shift variations between two collimated beams, derived by splitting light from a single source. A beamsplitter is used in order to split a light beam into two parts. The split beam is then recombined by a second beamsplitter. Based on the relative phase acquired by the beam along the two paths, the second beamsplitter will reflect the beam with an efficiency between 0 and 100%. The Mach-Zehnder interferometer also enables the determination of the wavelength of a laser beam, the ability to determine the refractive index of a transparent material and also to establish the refractive index of air.

III. Modelling and Simulation

A. WAVEGUIDE

In my design, I use Strip waveguide with 500nm width and 220nm height.

Here are the simulated waveguide profiles:

The MODE simulation results show us below that they are quasi-TE polarized with an effective index n of 2.442 for a wavelength of 1.55um for mode #1.

TE mode:

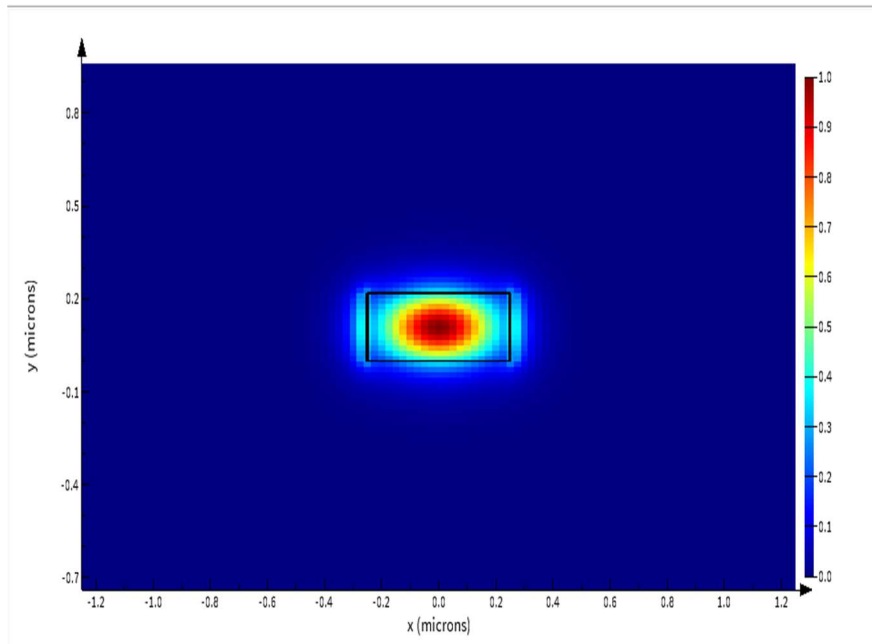


Figure1.Electric field intensity of TE mode in the waveguide

TM Mode:

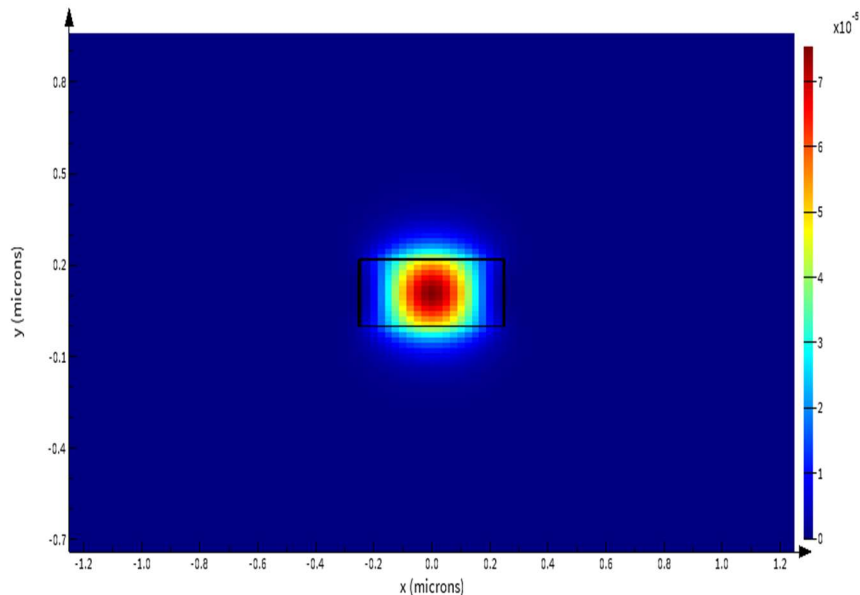


Figure2. Electric field intensity of TM mode in the waveguide

Variation of effective index n and group index ng with respect to wavelength. From the pictures we can infer that effective index decreases with wavelength and group index increases with respect to wavelength.

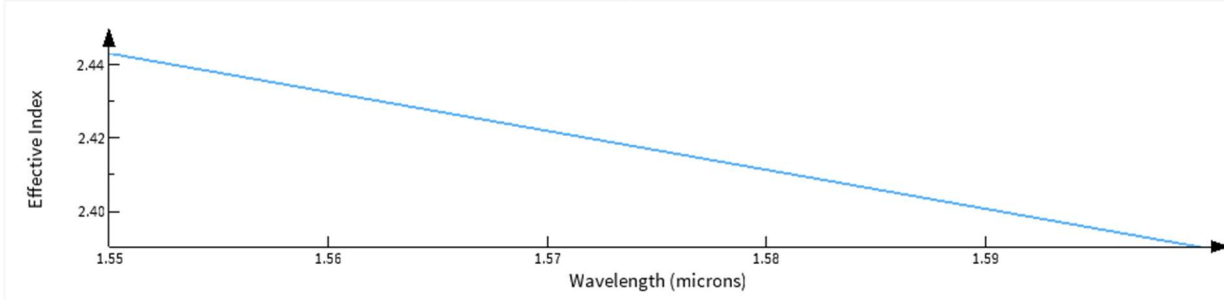


Figure 3. Wavelength vs. Effective Index from MODE simulations

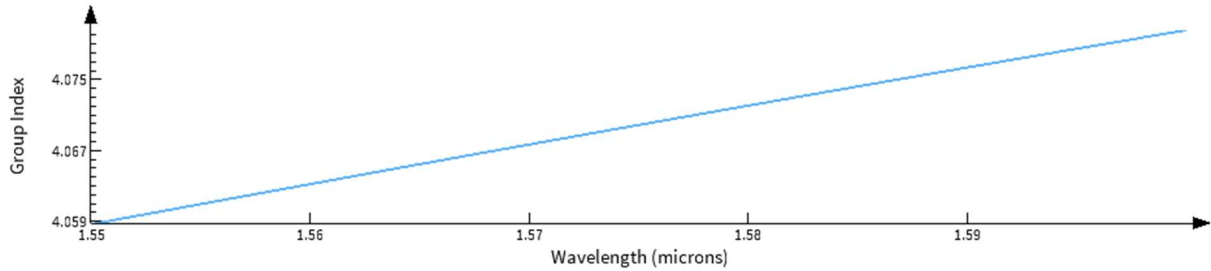


Figure 4. Wavelength vs. Group Index from MODE simulations

Using MATLAB, the compact model equation for the waveguide is obtained, which is a 2nd order polynomial.

$$neff(\lambda) = 2.44 - 1.1 * (\lambda - 1.55) - 0.04 * (\lambda - 1.55)^2$$

B. MACH-ZEHNDER INTERFEROMETER (MZI)

The transfer function of MZI is as follows:

$$T(MZI) = I_i * 2[1 + \cos(\beta \Delta L)]$$

where,

I_i = input intensity

β = Propagation constant of light

ΔL = Difference in waveguide length

Using Lumerical INTERCONNECT simulation and compact model waveguide generated from MODE simulation, here is how transfer function of MZI looks:

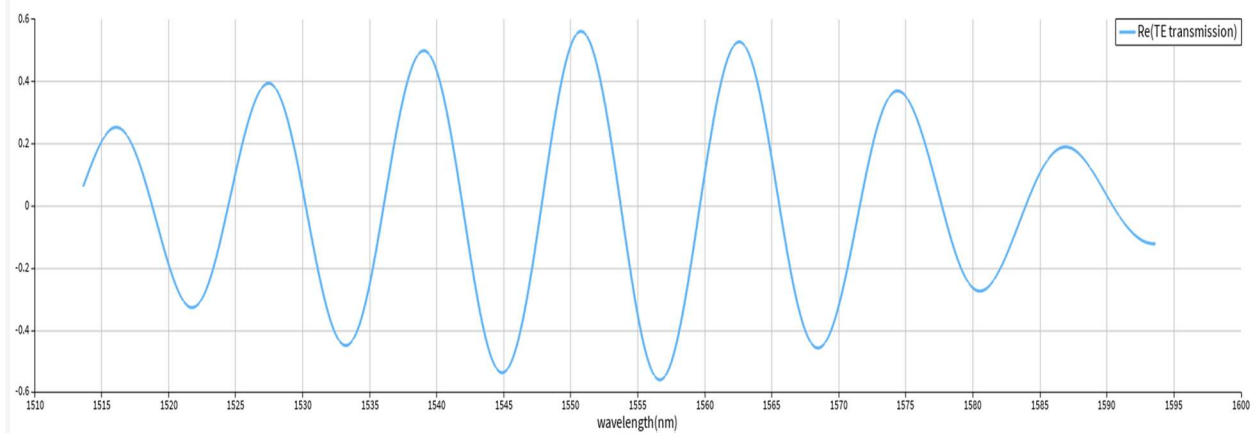


Figure 5. This is the Transfer function of an MZI using Y-branch and 2 waveguides of same length

C. FREE SPECTRAL RANGE

The Free Spectral Range of the Interferometer is calculated as

$$\text{FSR} = \lambda^2 / (n_0 \Delta L)$$

The Table below shows FSR simulated using Lumerical INTERCONNECT for different waveguide lengths done on the Klayout.

Width - 500

Delta L (um)	FSR (nm) mode 1, input1	FSR (nm) mode 1, input2
121.77	4.739	4.654
56.37	0.1035	9.974
46.32	0.1233	
126.36	4.545	

D.TRANSMISSION SPECTRUM

The picture below shows the TE spectrum of MZI with Delta L of 126.36um with both input1 and input2 in one graph based on Lumerical INTERCONNECT circuit simulations.

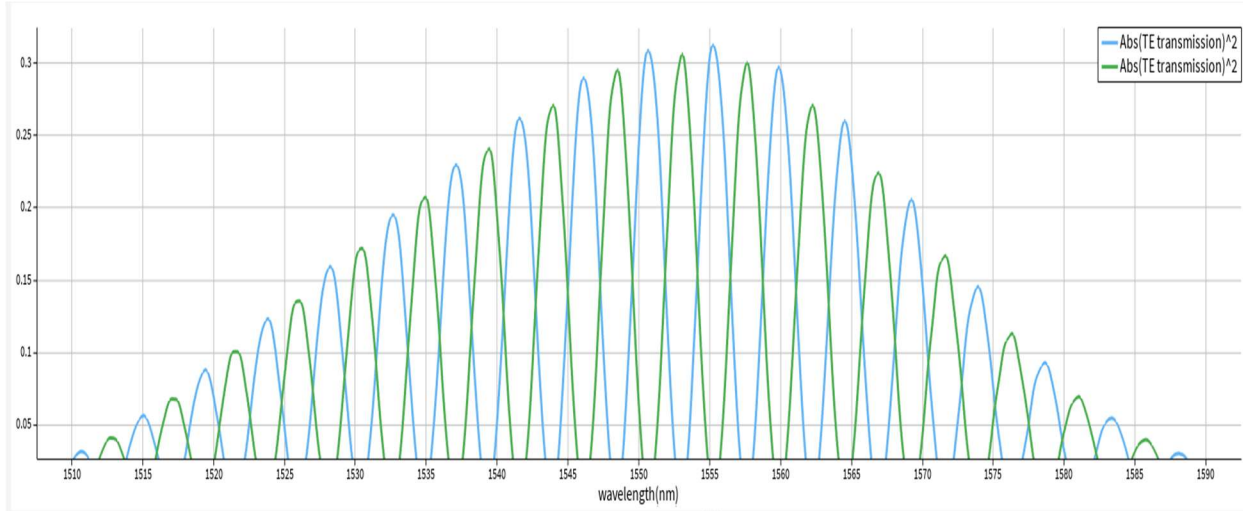


Figure6. MZI transmission spectrum using Y-branch for Mode 1, input 1 and input2

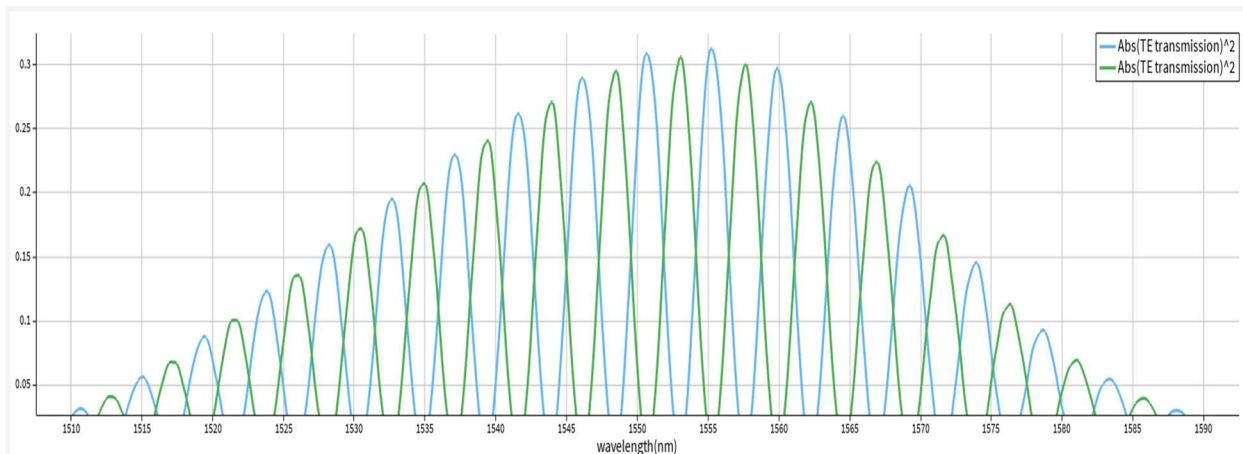


Fig 7. TE spectrum based on compact waveguide model from MODE and Optical 2-port s-parameter element with Y-Branch S-parameters populated. Waveguide length is 100 and 300um respectively.

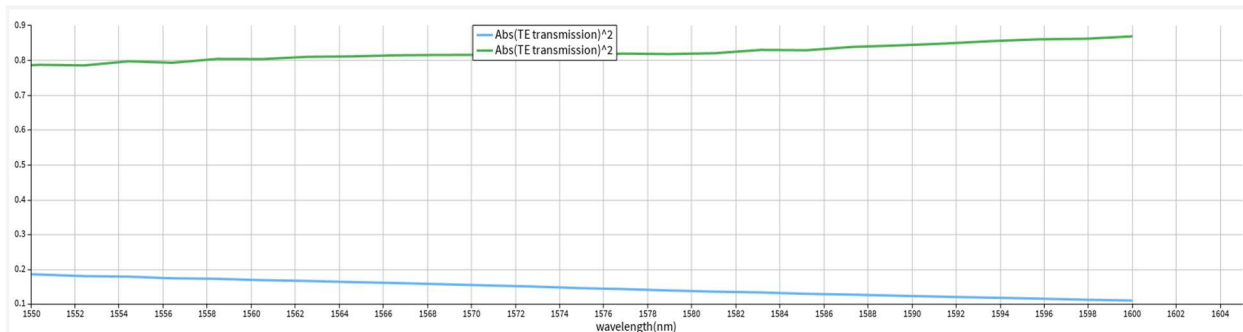


Fig8. 80-20 Adiabatic splitter transmission spectrum

E. IMBALANCED MZI INTERFEROMETER

For different levels of interference in MZI, an unequal length is introduced between the branches as indicated in Fig 9.

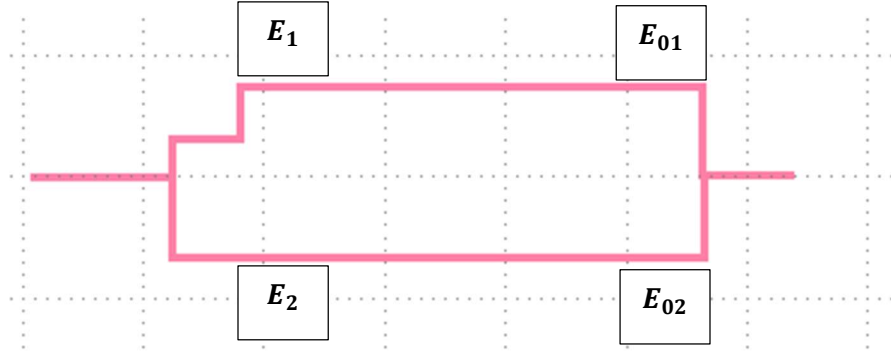


Fig 9. Imbalanced MZI

The upper and lower waveguides have different lengths, L_1 and L_2 with different effective indices n_1 and n_2 . Hence the propagation constant for these two branches is defined as:

$$\beta_1 = 2\pi n_1 / \lambda$$

$$\beta = 2\pi n_2 / \lambda$$

The vectorial electrical field at the input of the MZI is represented by E_1 and E_2 . At the output of the beam-splitter, the complex electrical fields at the upper and lower branches are given by,

$$E_1 = E_2 = \frac{1}{\sqrt{2}} E_i$$

The electrical fields at the input of the beam-combiner can be described by,

$$E_{01} = E_i e(-j\beta_1 L_1 - \alpha_1 L_1) \quad \text{-----} > (1)$$

$$E_{02} = E_i e(-j\beta_2 L_2 - \alpha_2 L_2) \quad \text{-----} > (2)$$

When light is combined in the y-branch at the output, output intensity is defined as follows,

$$E_0 = \frac{1}{\sqrt{2}} \cdot [E_{01} + E_{02}] \quad \text{-----} \rightarrow (3)$$

Combining eqns (1) and (2) in eqn (3),

$$E_0 = \frac{1}{2} \cdot [E_i e(-j\beta_1 L_1 - \alpha_1 L_1) + E_i e(-j\beta_2 L_2 - \alpha_2 L_2)] \quad \text{-----} > (4)$$

Finally light intensity is squared power of intensity amplitude,

$$I_0 = \frac{1}{2} \cdot |[I_1 e(-j\beta_1 L_1 - \alpha_1 L_1) + I_2 e(-j\beta_2 L_2 - \alpha_2 L_2)]|^2 \quad (5)$$

Solving for I_0 ,

$$I_0 = \frac{1}{2} \cdot I_i (1 + \cos \beta \Delta L)$$

where $\Delta L = L_1 - L_2$, and $\beta_1 = \beta_2 = \beta$

The spacing between the adjacent peaks is defines as free spectral range,

$$\text{FSR} = \lambda^2 / \Delta L \cdot n_g(\lambda)$$

IV. MZI Design based on Layout and Circuit Simulation

The following table illustrates MZI1 using bdc_te couplers and corresponding FSR is calculated for different lengths of the waveguide

EBeam_bdc_te1550	L1	L2	Delta L (um)	FSR (nm) mode 1, input1	FSR (nm) mode 1, input2
MZI1	43.668	300	256.332	2.25	2.29

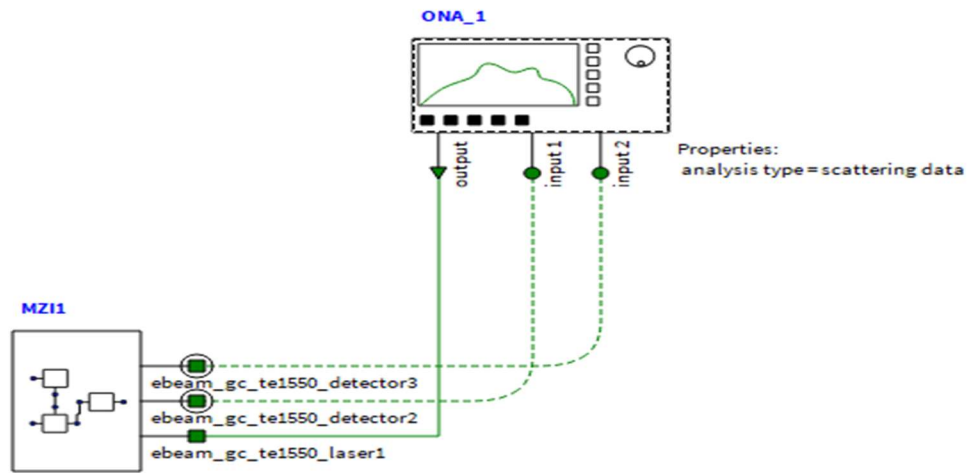


Figure10. Lumeral Interconnect simulations

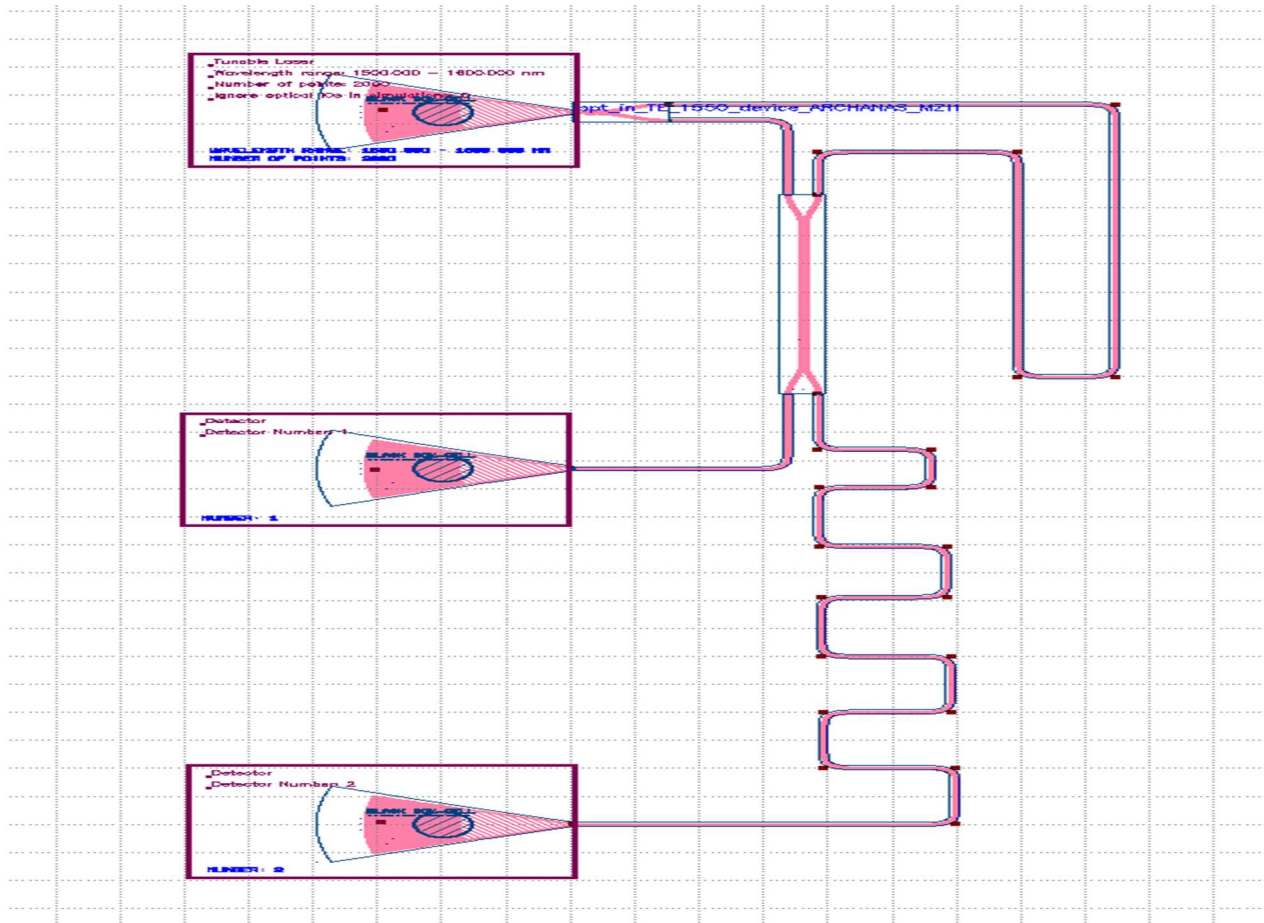


Figure 11. Layout of MZI1 using Bdc_te couplers

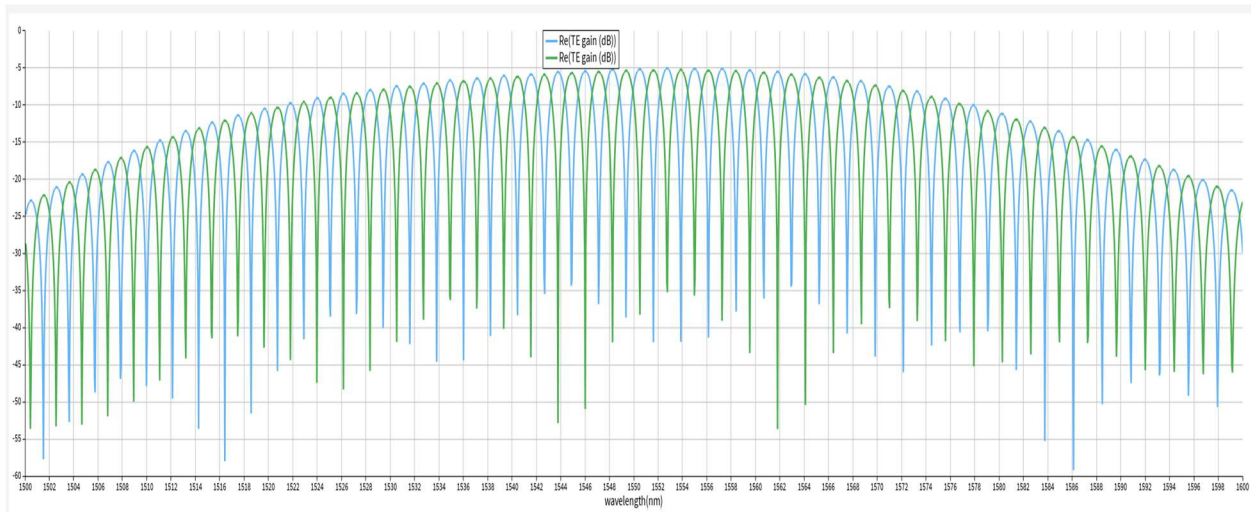


Figure 12.TE Gain a) Blue(input1) b) Green(input2)

The TE Gain observed at 1550nm wavelength for input1 is -5.98dB and for input2 is -12.712dB

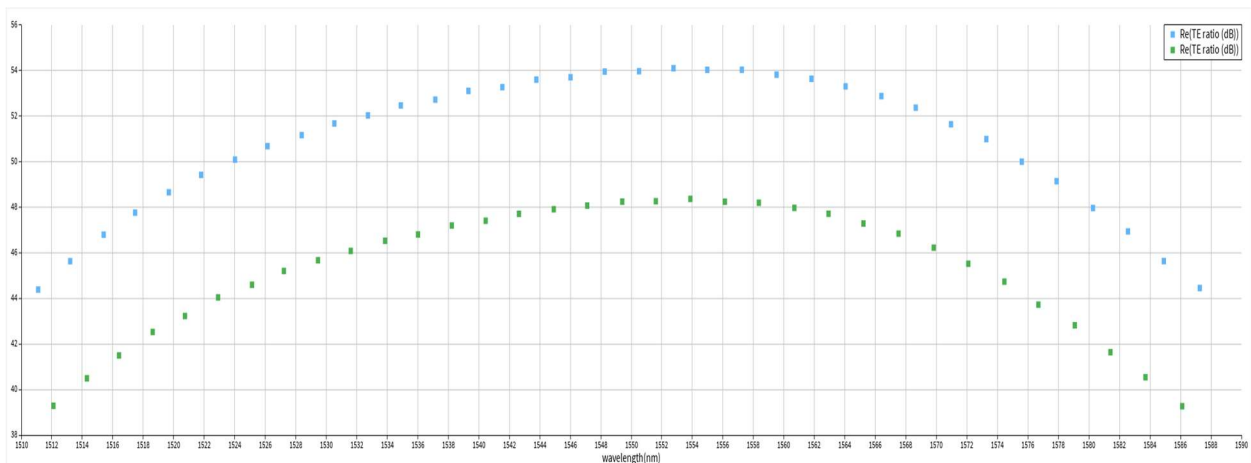


Figure 13.TE Ratio/Extinction Ratio a) Blue(input1) b)Green(input2)

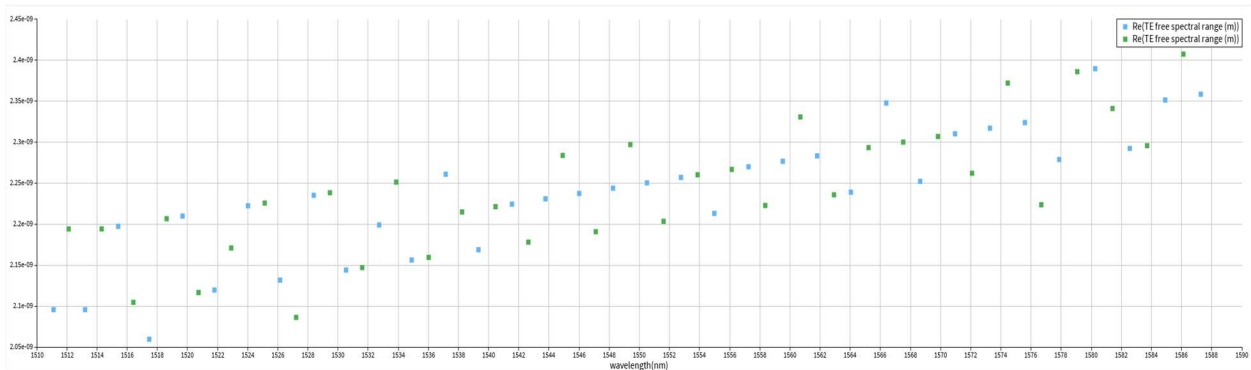


Figure 14. Free Spectral Range a) Blue(input1) b) Green(input2)

The following table illustrates MZI1 using bdc_te couplers and corresponding FSR is calculated for different lengths of the waveguide

EBeam_bdc_te1550	L1	L2	Delta L (um)	FSR (nm) mode 1, input1	FSR (nm) mode 1, input2
MZI2	220	100.001	119.99	4.7	

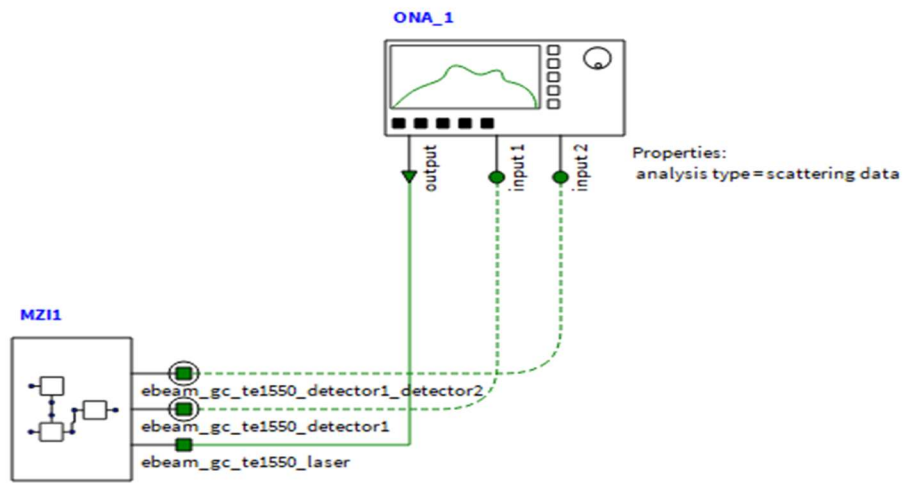


Figure 15. Simulation with Lumerical INTERCONNECT using bdc_te_1550

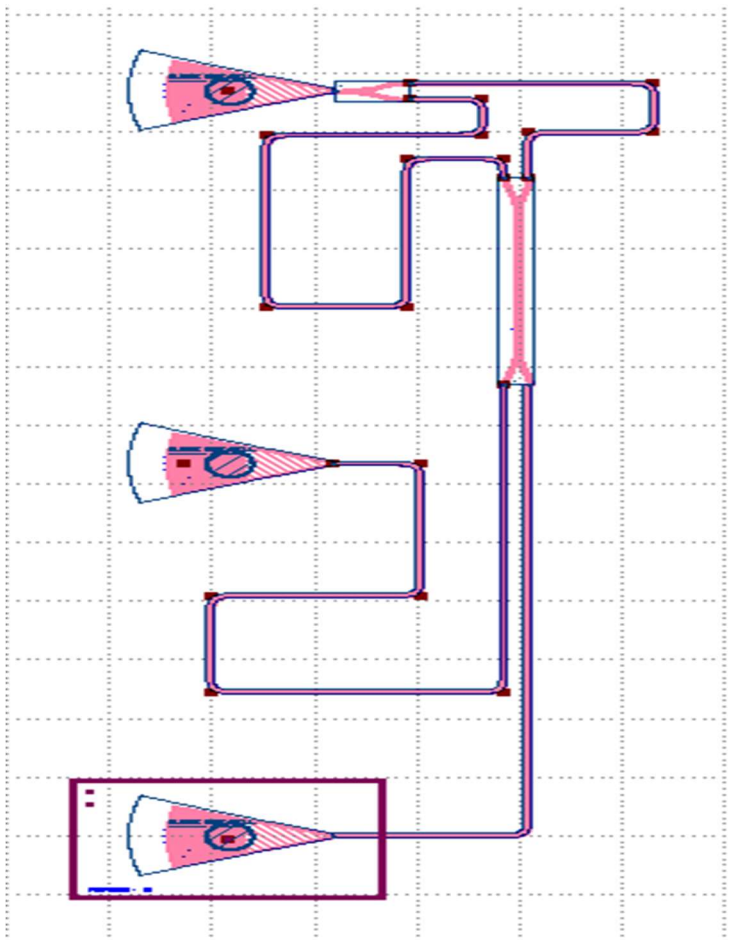


Figure 16. KLayout using bdc_te1550 for MZI2

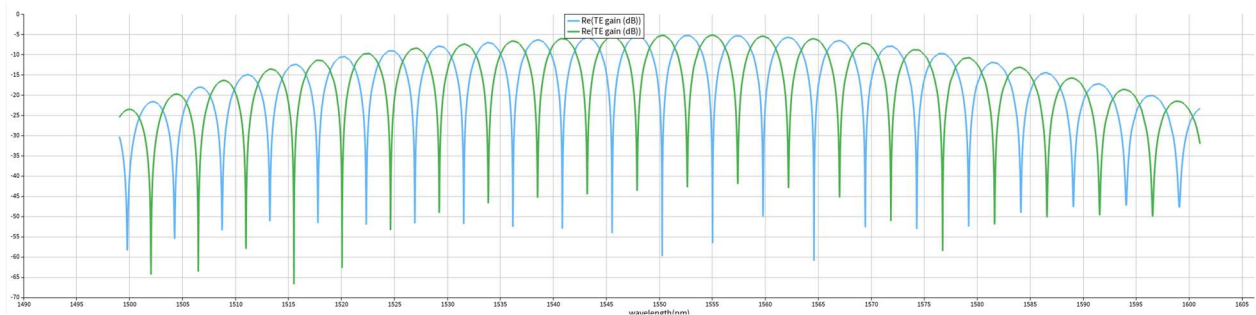


Figure 17.TE Gain a) Blue(input1) b) Green(input2)

The TE Gain observed at 1550nm wavelength for input1 is -21.145dB and for input2 is -5.438dB

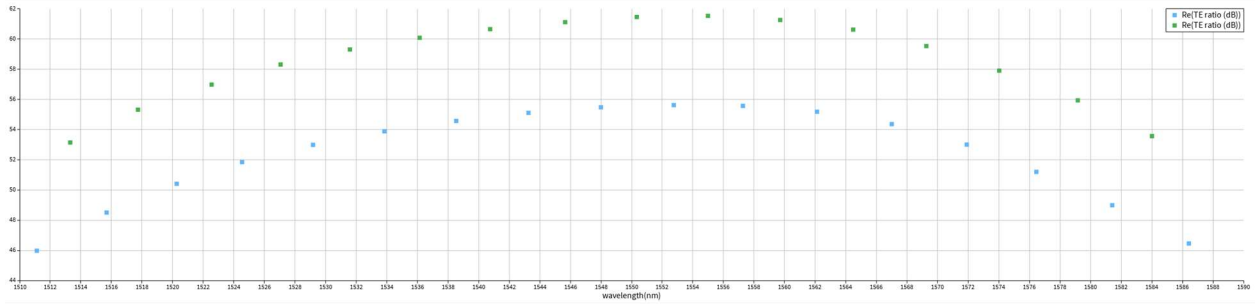


Figure 18.TE Ratio/Extinction Ratio a) Blue(input1) b)Green(input2)

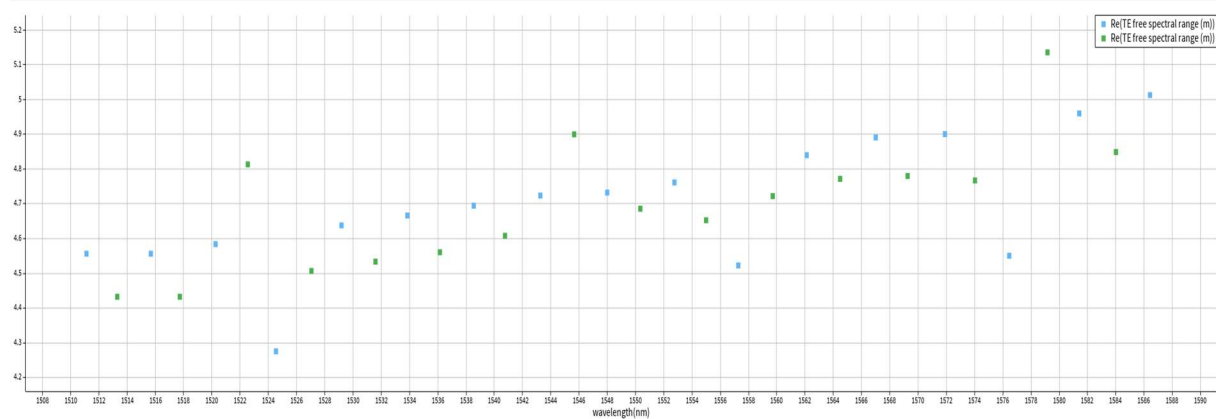


Figure 19. Free Spectral Range a) Blue(input1) b) Green(input2)

The following table illustrates MZI3 using dc_te couplers and corresponding FSR is calculated for different lengths of the waveguide

EBeam_dc_te1550	L1(um)	L2(um)	Delta L (um)	FSR (nm) mode 1, input1
MZI3	61.558	320	258.442	2.213

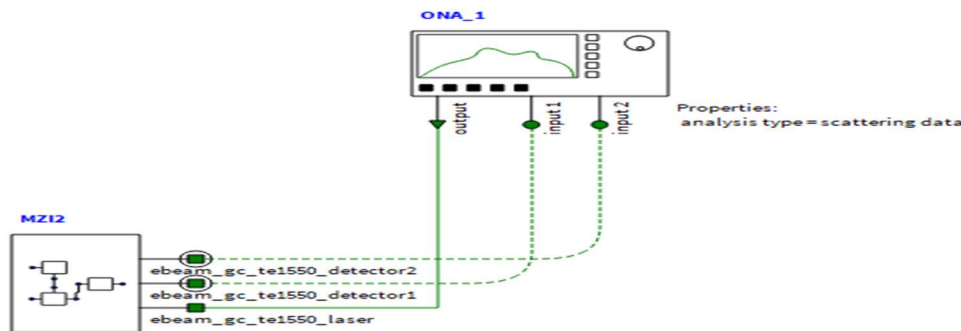


Figure 20. Simulation with Lumerical INTERCONNECT using dc_te_1550

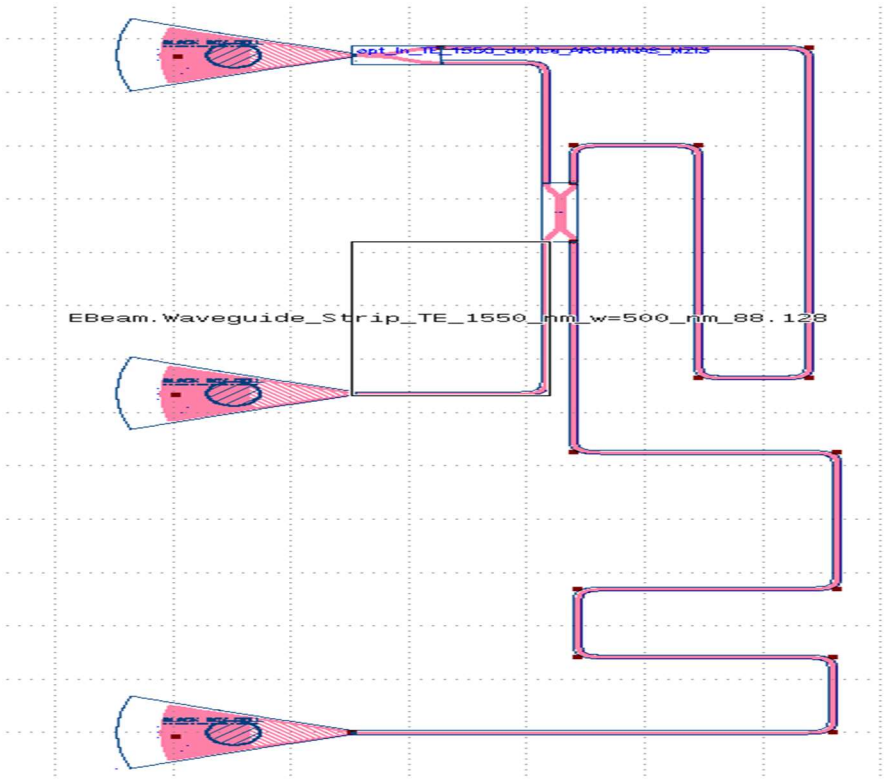


Figure 21. KLayout using dc_te1550 for MZI3

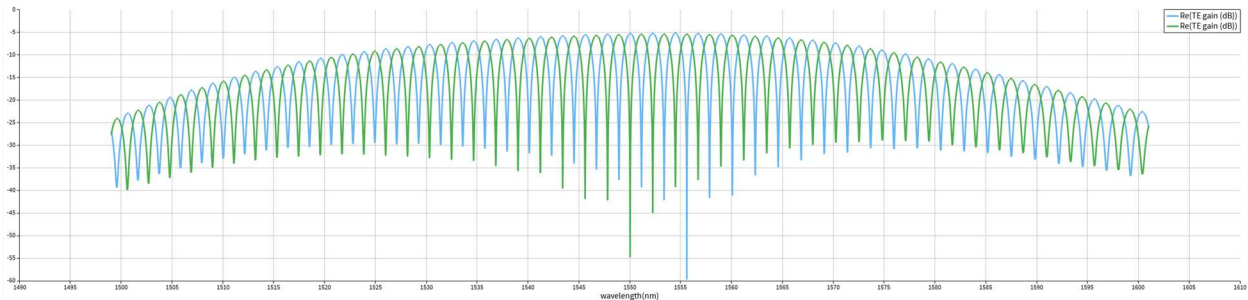


Figure 22.TE Gain a) Blue(input1) b) Green(input2)

The TE Gain observed at 1550nm wavelength for input1 is -5.29dB and for input2 is -29.78dB

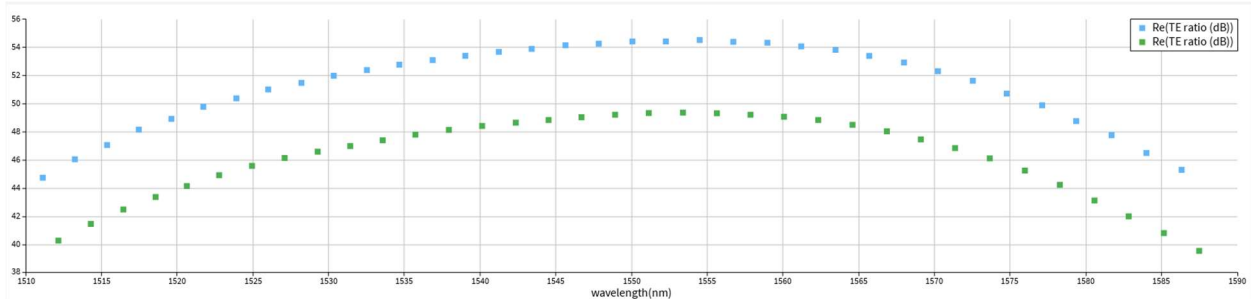


Figure 23. TE Ratio/Extinction Ratio a) Blue(input1) b) Green(input2)

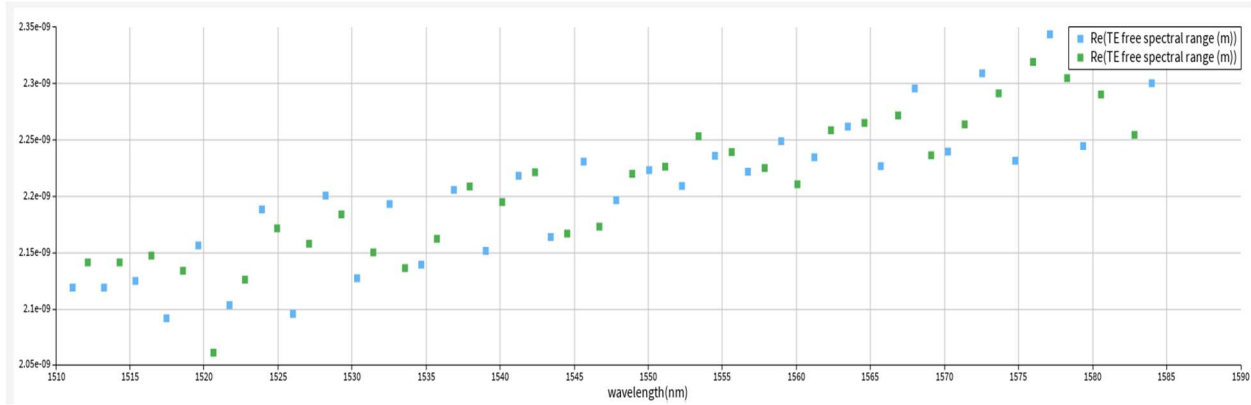


Figure 24. Free Spectral Range a) Blue(input1) b) Green(input2)

The following table illustrates MZI4 using adiabatic splitter and corresponding FSR is calculated for different lengths of the waveguide

EBeam_adiabatic_te1550	L1(um)	L2(um)	Delta L (um)	FSR (nm) mode 1, input1
MZI4	38.298	222.012	183.714	3.1

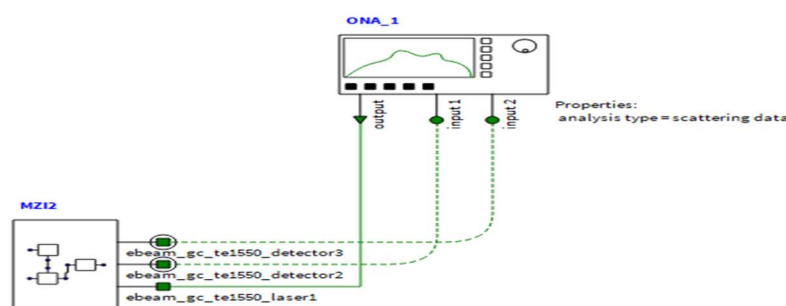


Figure 25. Figure 19. Simulation with Lumerical INTERCONNECT using dc_te_1550

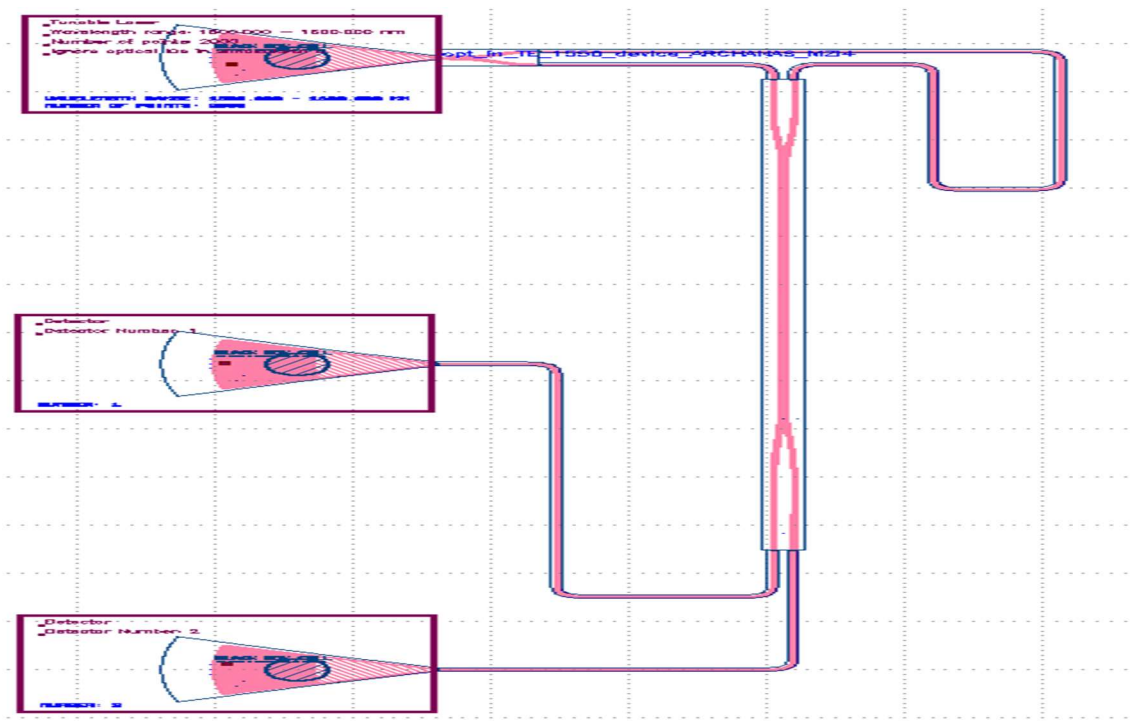


Figure 26. Figure 20. KLayout using adiabatic te1550

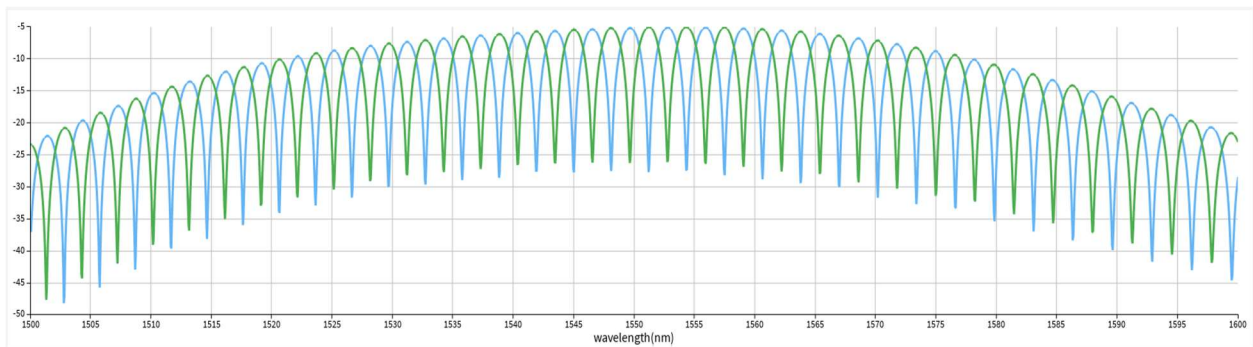


Figure 27. TE Gain a) Blue(input1) b) Green(input2)

The TE Gain observed at 1550nm wavelength for input1 is -5.38dB and for input2 is -13.177dB

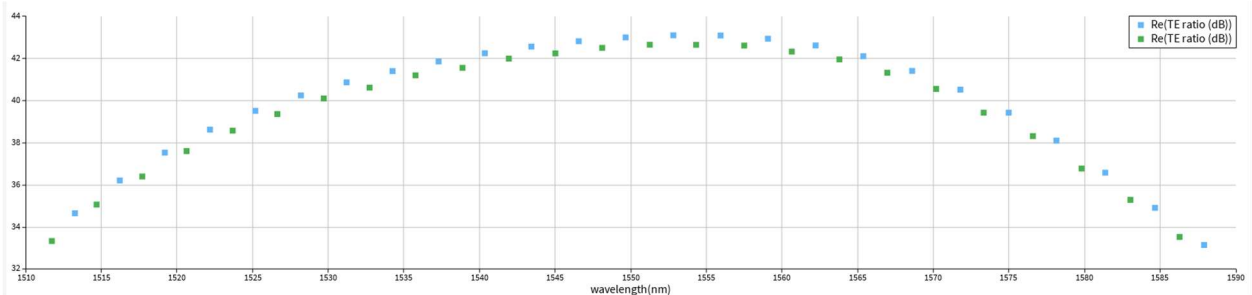


Figure 28.TE Ratio/Extinction Ratio a) Blue(input1) b) Green(input2)

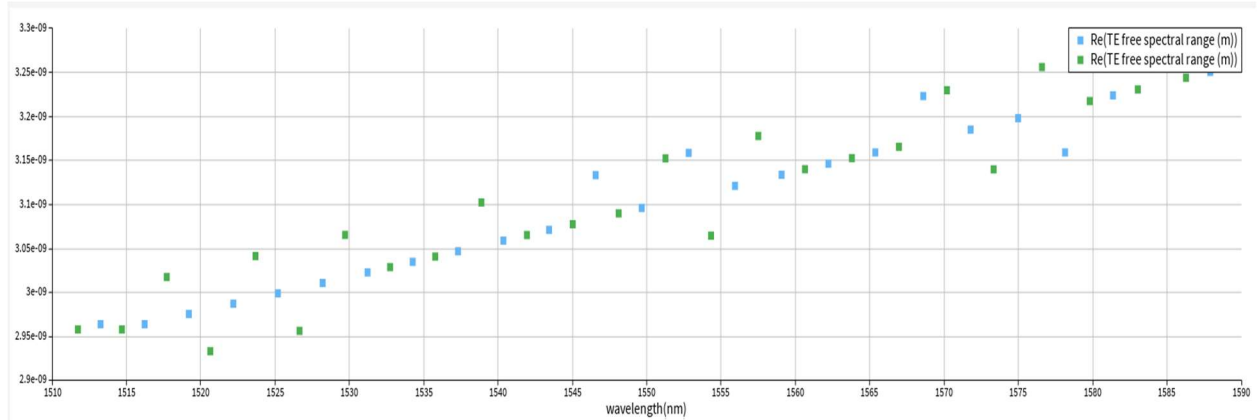


Figure 29. Free Spectral Range a) Blue(input1) b) Green(input2)

V. Corner Analysis – MODE Simulations

The below table captures group index data for TE 1550 500 X 220 nm type waveguide for different length and width of the waveguide. This was simulated in MODE manually and group index was calculated for each case.

x, y represents length and width of the waveguide

x, y	Waveguide dimensions	Group index, ng
0.47,0.215	470 X 215	4.256
0.48,0.216	480 X 216	4.236
0.49,0.217	490 X 217	4.216
0.5,0.218	500 X 218	4.2
0.505,0.219	505 X 219	4.193
0.51,0.22	510 X 220	4.185
0.51,0.221	510 X 221	4.186
0.51,0.222	510 X 222	4.187
0.51,0.223	510 X 223	4.188

Using above group index value ng, FSR can be calculated. The below table captures FSR calculated manually using,

$$\text{FSR} = \lambda^2 / (\Delta L * n_g) \text{ where } \lambda = 1550\text{nm}$$

ng	FSR (nm)
4.256	5.644
4.236	5.671
4.216	5.69
4.20	5.720
4.193	5.729
4.185	5.74
4.186	5.739
4.187	5.737
4.188	5.736

VI. Corner Analysis - Monte Carlo Simulations

- 1) Below are the results of Monte Carlo simulations done on 50 wafers and 10 dies within each wafer

Based on layout of MZI1 Delta L – 256um

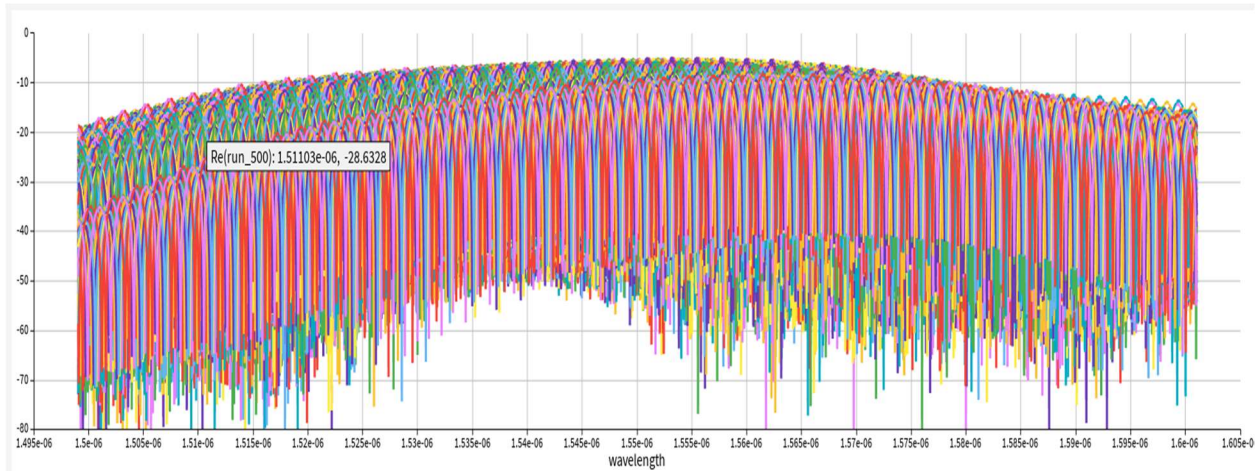


Figure 30. MZI Transfer Function using Monte-Carlo simulation for MZI1 Design

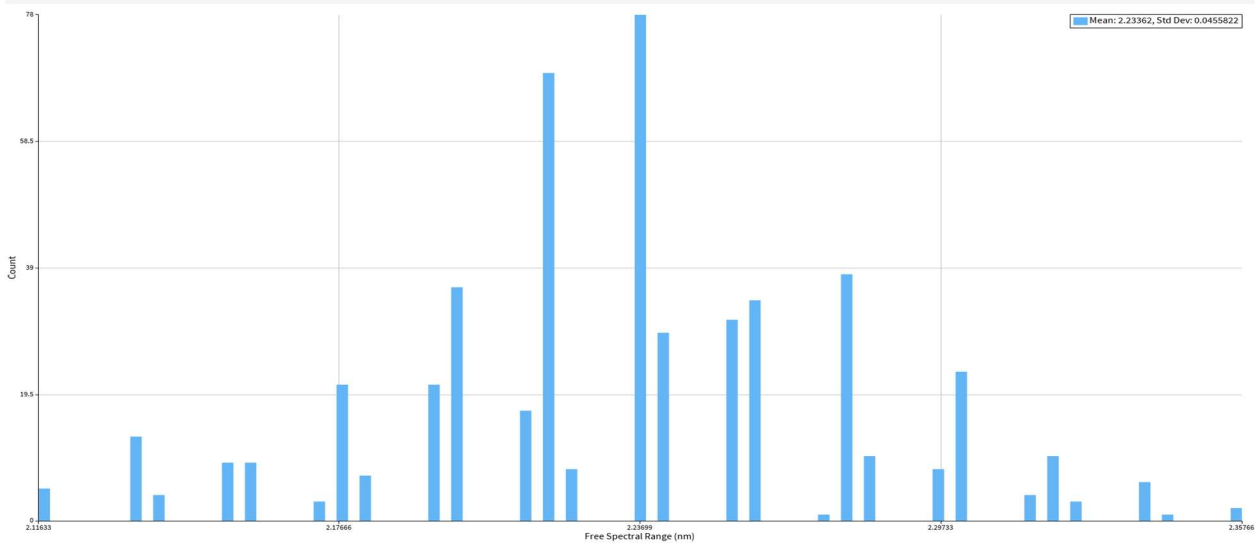


Figure 31. Histogram – FSR using Monte-Carlo simulation for MZI1 Design

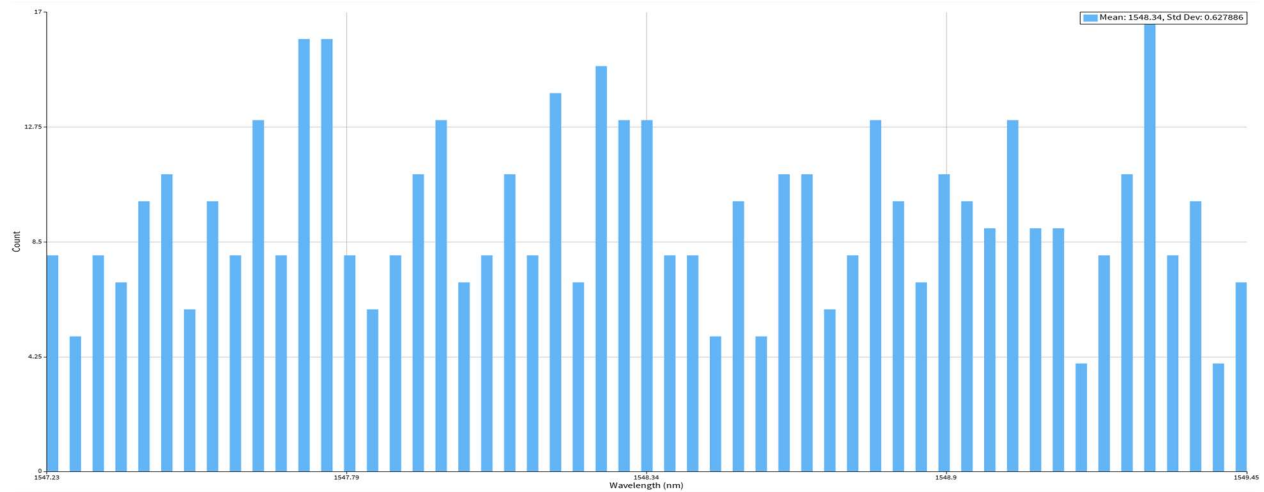


Figure 32. Histogram – Peak wavelength using Monte-Carlo simulation for MZI1 Design

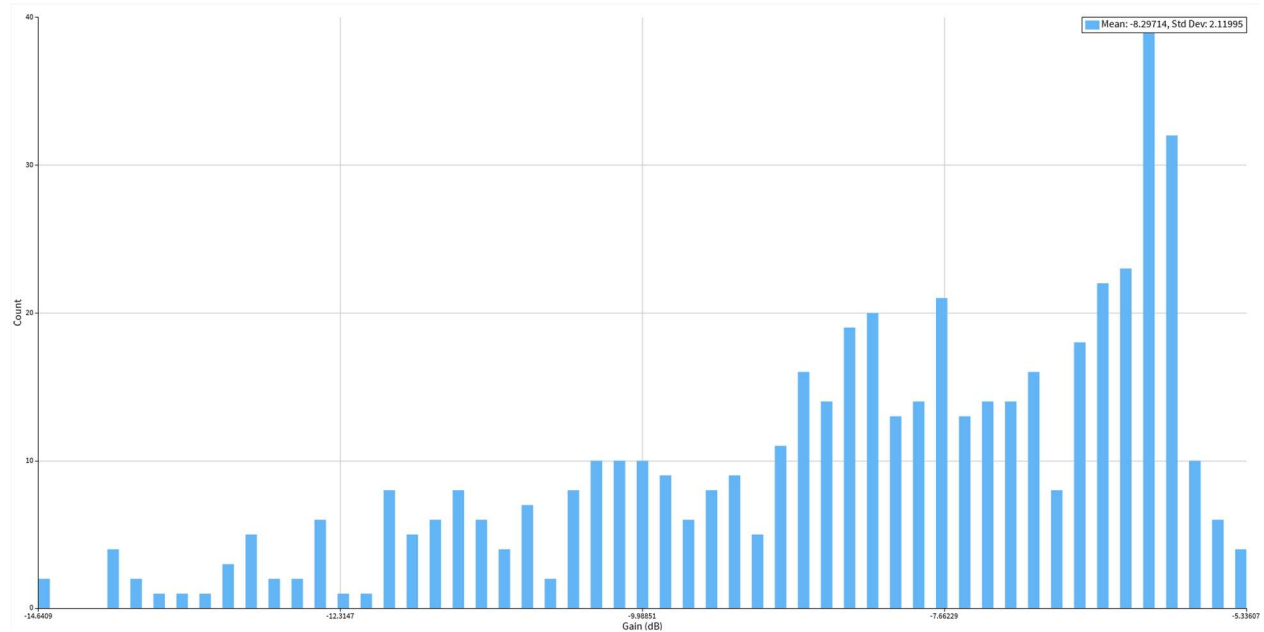


Figure 33. Histogram – Peak Gain using Monte-Carlo simulation for MZI1 Design

- 2) Below are the results of Monte Carlo simulations done on 50 wafers and 10 dies within each wafer

Based on layout of MZI2 Delta L – 120um

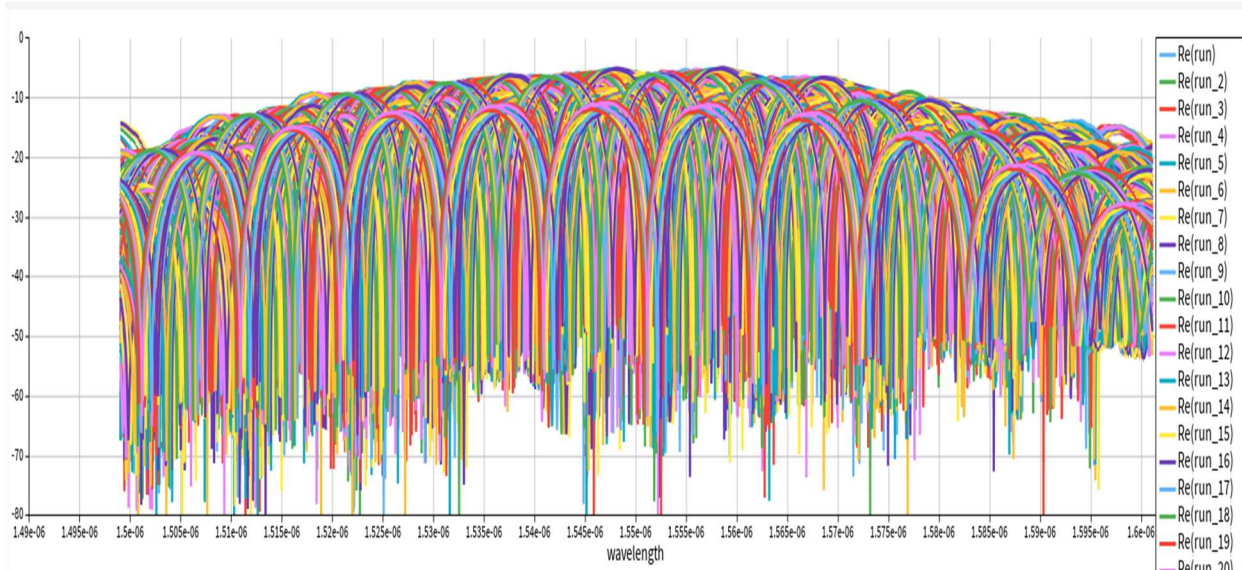


Figure 34. MZI Transfer Function using Monte-Carlo simulations for MZI2 Design

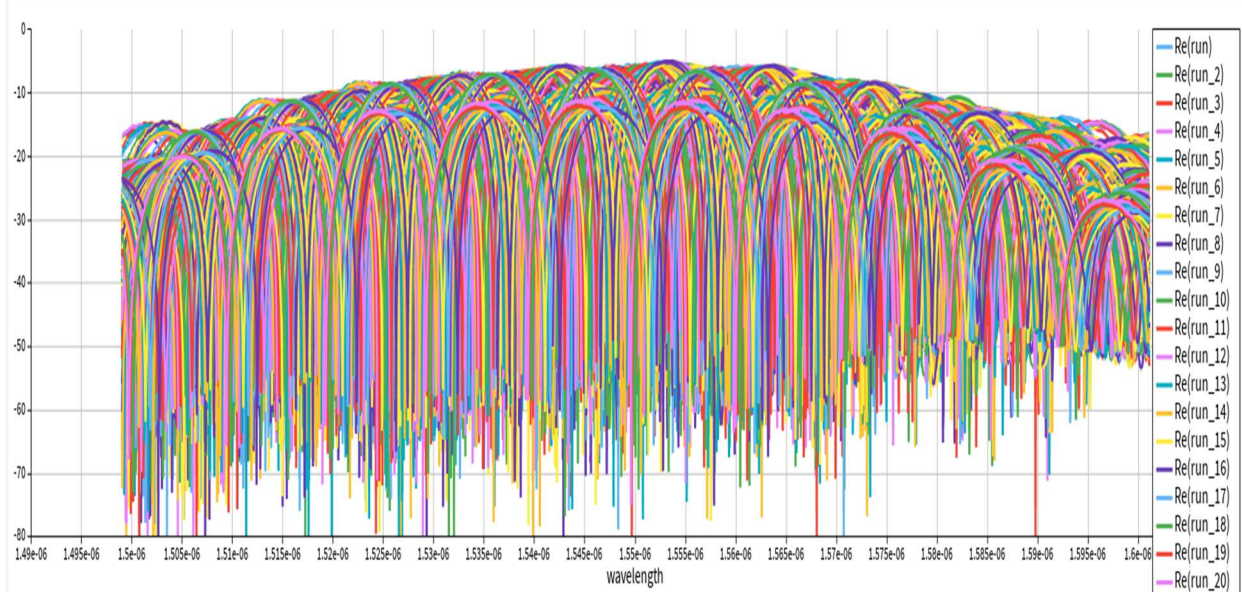


Figure 35. MZI Transfer Function using Monte-Carlo simulations for MZI2 Design

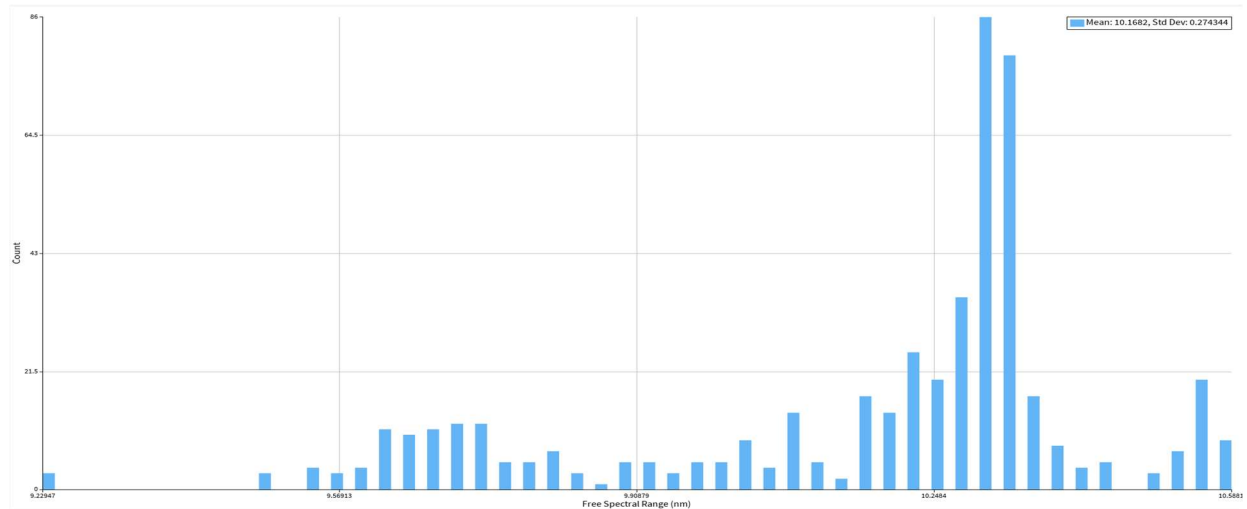


Figure 36. Histogram – FSR using Monte-Carlo simulations for MZI2 Design

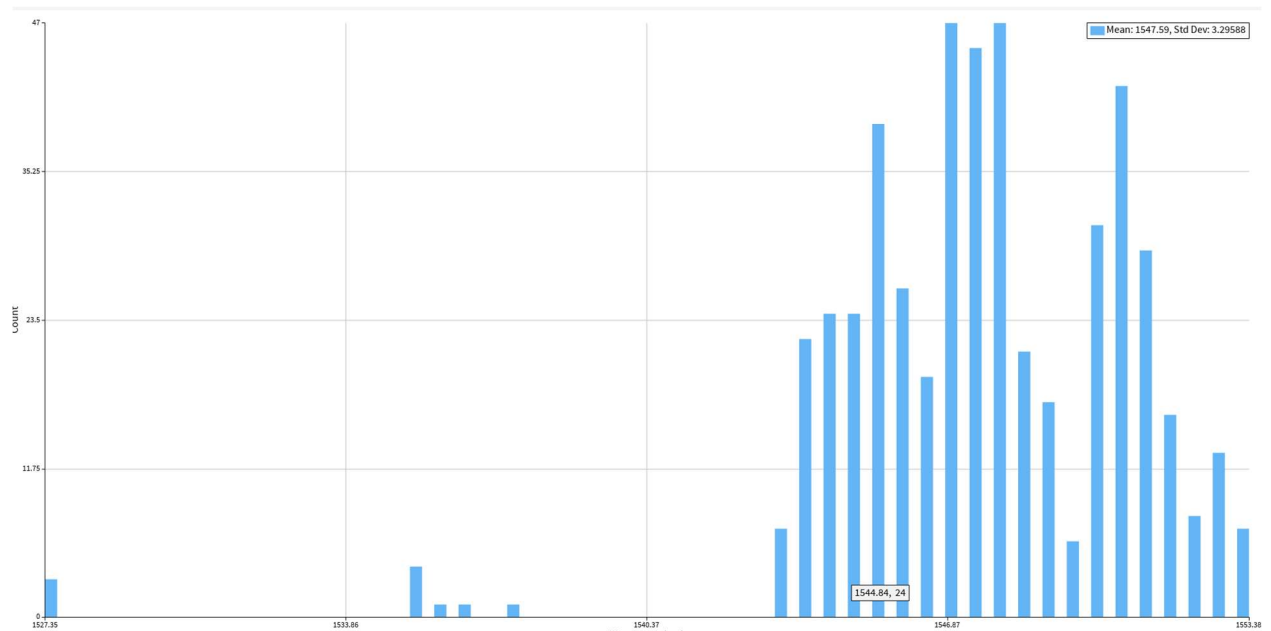


Figure 37. Histogram – Peak wavelength using Monte-Carlo simulations for MZI2 Design

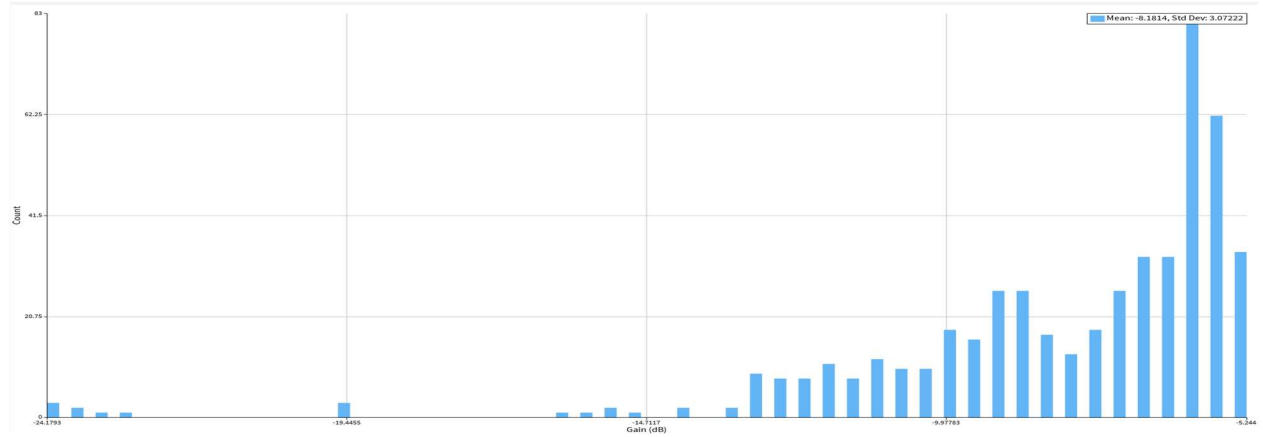


Figure 38. Histogram – Peak Gain using Monte-Carlo simulations for MZI2 Design

3) Below are the results of Monte Carlo simulations done on 50 wafers and 10 dies within each wafer

Based on layout of MZI3

EBeam_dc_te1550	L1(um)	L2(um)	Delta L (um)	FSR (nm) mode 1, input1	FSR (nm) mode 1, input2
	61.558	320	258.442	2.213	1.917
Case i)	88.128	386.418	298.29		

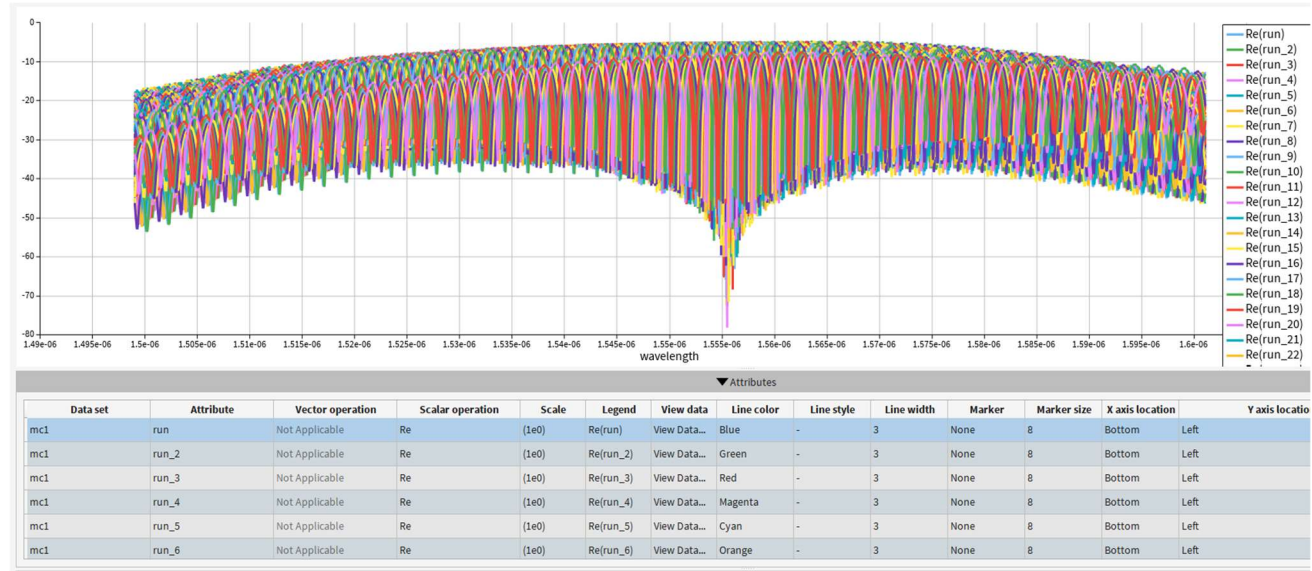


Figure 39. MZI Transfer function using Monte-Carlo simulations for MZI3 Design

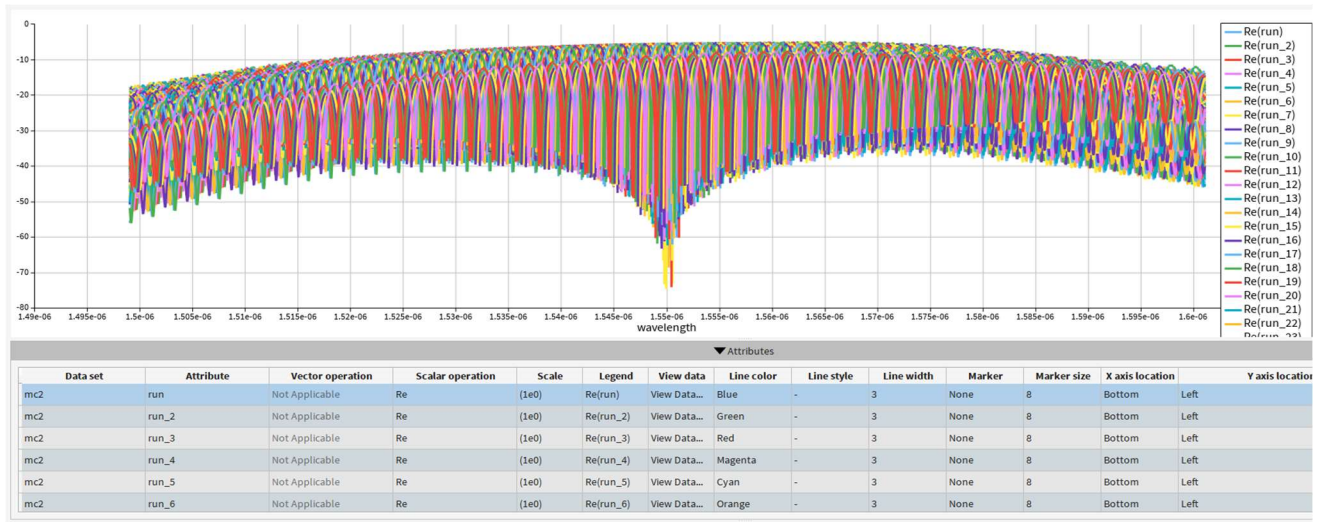


Figure 40. MZI Transfer function using Monte-Carlo simulations for MZI3 Design

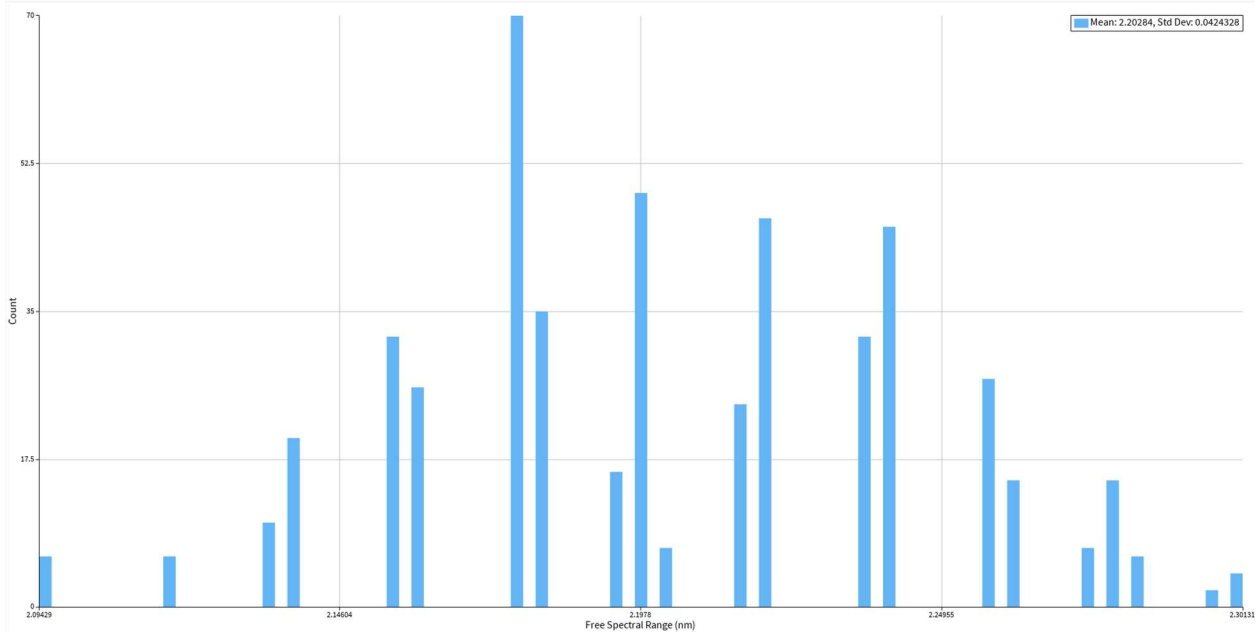


Figure 41. Histogram – FSR using Monte-Carlo simulations for MZI3 Design

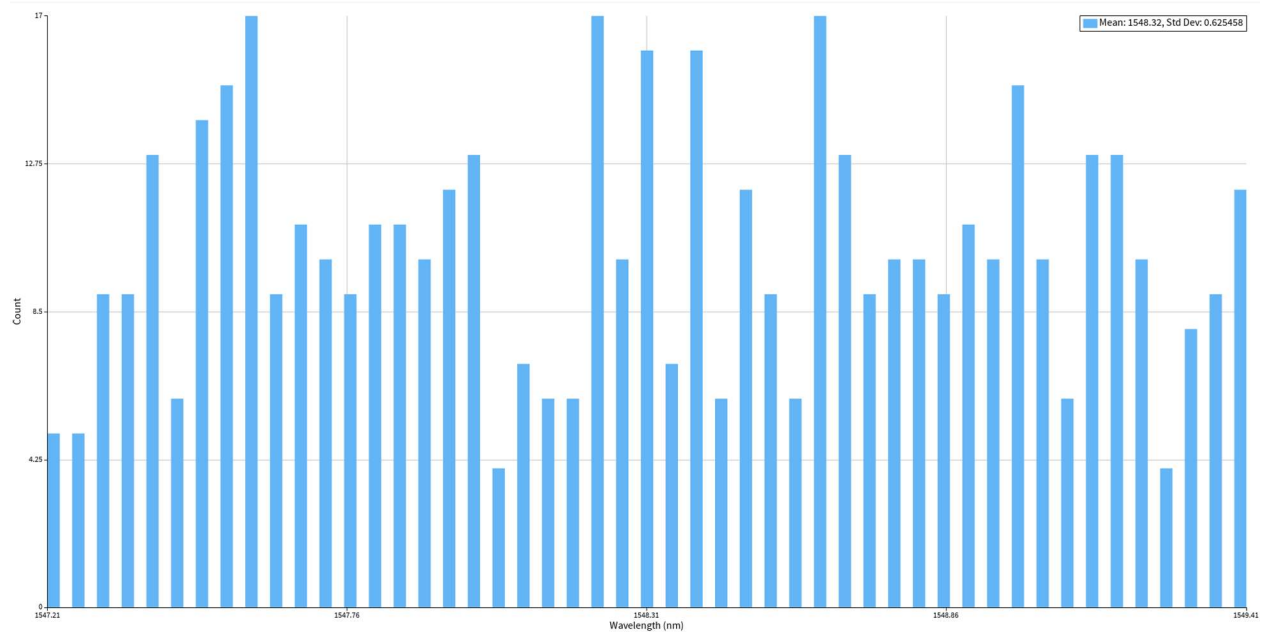


Figure 42. Histogram – Peak wavelength using Monte-Carlo simulations for MZI3 Design

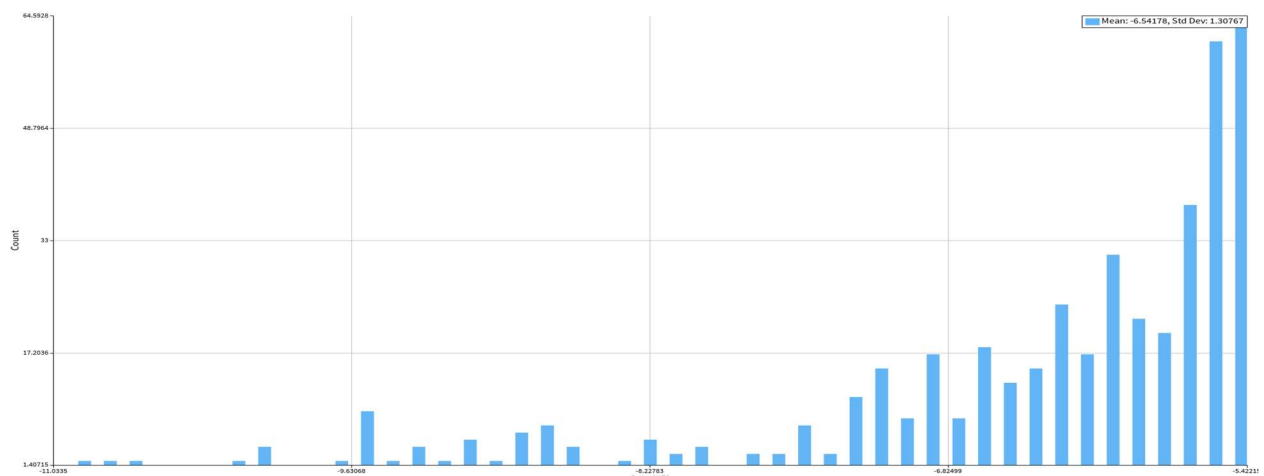


Figure 43. Histogram – Peak Gain using Monte-Carlo simulations for MZI3 Design

VII. Measurement Data

1. SUMMARY OF THE FABRICATION DESCRIPTION:

Fabrication is performed at one or more of these: Applied Nanotools and Washington Nanofabrication Facility. The following are the process descriptions.

Applied Nanotools, Inc. Nano SOI process:

The photonic devices were fabricated using the Nano SOI MPW fabrication process by Applied Nanotools Inc. (<http://www.appliednt.com/nanosoi>; Edmonton, Canada) which is based on direct-write 100 keV electron beam lithography technology. Silicon-on-insulator wafers of 200 mm diameter, 220 nm device thickness and 2 μm buffer oxide thickness are used as the base material for the fabrication. The wafer was pre-diced into square substrates with dimensions of 25x25 mm, and lines were scribed into the substrate backides to facilitate easy separation into smaller chips once fabrication was complete. After an initial wafer clean using piranha solution (3:1 H₂SO₄:H₂O₂) for 15 minutes and water/IPA rinse, hydrogen silsesquioxane (HSQ) resist was spin-coated onto the substrate and heated to evaporate the solvent. The photonic devices were patterned using a JEOL JBX-8100FS electron beam instrument at The University of British Columbia. The exposure dosage of the design was corrected for proximity effects that result from the backscatter of electrons from exposure of nearby features. Shape writing order was optimized for efficient patterning and minimal beam drift. After the e-beam exposure and subsequent development with a tetramethylammonium sulfate (TMAH) solution, the devices were inspected optically for residues and/or defects. The chips were then mounted on a 4" handle wafer and underwent an anisotropic ICP-RIE etch process using chlorine after qualification of the etch rate. The resist was removed from the surface of the devices using a 10:1 buffer oxide wet etch, and the devices were inspected using a scanning electron microscope (SEM) to verify patterning and etch quality. A 2.2 μm oxide cladding was deposited using a plasma-enhanced chemical vapour deposition (PECVD) process based on tetraethyl orthosilicate (TEOS) at 300°C. Reflectometry measurements were performed throughout the process to verify the device layer, buffer oxide and cladding thicknesses before delivery.

Washington Nanofabrication Facility (WNF) silicon photonics process

The devices were fabricated using 100 keV Electron Beam Lithography [1]. The fabrication used silicon-on-insulator wafer with 220 nm thick silicon on 3 μm thick silicon dioxide. The substrates were 25 mm squares diced from 150 mm wafers. After a solvent rinse and hot-plate dehydration bake, hydrogen silsesquioxane resist (HSQ, Dow-Corning XP-1541-006) was spin-coated at 4000 rpm, then hotplate baked at 80 °C for 4 minutes. Electron beam lithography was performed using a JEOL JBX-6300FS system operated at 100 keV energy, 8 nA beam current, and 500 μm exposure field size. The machine grid used for shape placement was 1 nm, while the beam stepping grid, the spacing between dwell points during the shape writing, was 6 nm. An exposure dose of 2800 $\mu\text{C}/\text{cm}^2$ was used. The resist was developed by immersion in 25% tetramethylammonium hydroxide for 4 minutes, followed by a flowing deionized water rinse for 60 s, an isopropanol rinse for 10 s, and then blown dry with nitrogen. The silicon was removed from unexposed areas using inductively coupled plasma etching in an Oxford Plasmalab System 100, with a chlorine gas flow of 20 sccm, pressure of 12 mT, ICP power of 800 W, bias power of 40 W, and a platen temperature of

20 °C, resulting in a bias voltage of 185 V. During etching, chips were mounted on a 100 mm silicon carrier wafer using perfluoropolyether vacuum oil. Cladding oxide was deposited using plasma enhanced chemical vapor deposition (PECVD) in an Oxford Plasmalab System 100 with a silane (SiH_4) flow of 13.0 sccm, nitrous oxide (N_2O) flow of 1000.0 sccm, high-purity nitrogen (N_2) flow of 500.0 sccm, pressure at 1400mT, high-frequency RF power of 120W, and a platen temperature of 350C. During deposition, chips rest directly on a silicon carrier wafer and are buffered by silicon pieces on all sides to aid uniformity.

Measurement description:

To characterize the devices, a custom-built automated test setup [2, 6] with automated control software written in Python was used [3]. An Agilent 81600B tunable laser was used as the input source and Agilent 81635A optical power sensors as the output detectors. The wavelength was swept from 1500 to 1600 nm in 10 pm steps. A polarization maintaining (PM) fibre was used to maintain the polarization state of the light, to couple the TE polarization into the grating couplers [4]. A 90° rotation was used to inject light into the TM grating couplers [4]. A polarization maintaining fibre array was used to couple light in/out of the chip [5].

VIII. Data Analysis using MATLAB

2.1 Below is the summary of data collected using MATLAB for MZI1 Design which has a dL of 256.332um.

Below plots were done in MATLAB by correcting Baseline data and fitting the MZI spectrum with experimental data

MZI1 (dL = 256.332um)	Channel 1	Channel 2
FSR	2.245nm	2.23nm
Ng_av	4.0945	4.122
x-fit	2.3963 -1.1590 -0.0153 0.0010 0.5102	2.4219 -1.1415 -0.0144 0.0024 1.1746
R^2	0.9068	0.9345
Ng0	4.1741	4.174
Waveguide parameters at wavelength	1.5338 um	1.5327 um
Dispersion	156.8012 [ps/nm/km]	144.3218

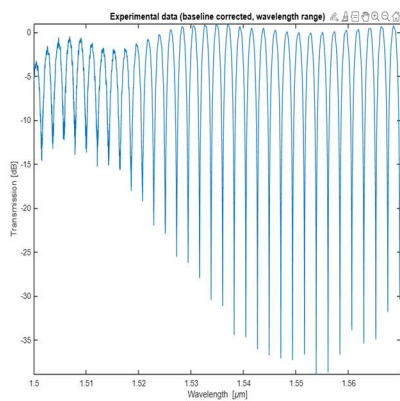


Figure 44. Baseline corrected exp. data

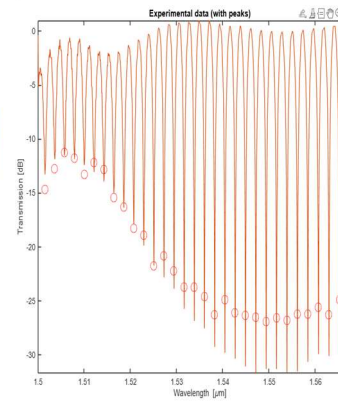


Figure 45. Exp. data with peaks

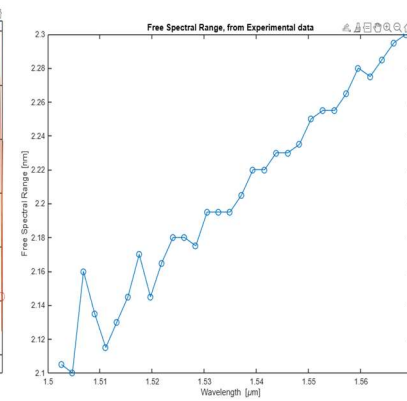


Figure 46. FSR from exp. data

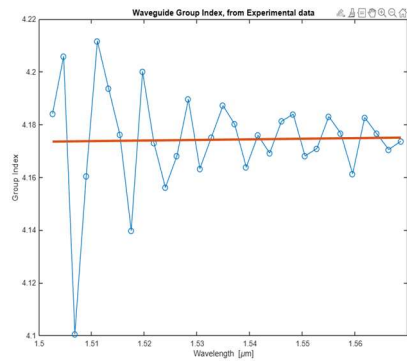


Figure 47. Group index vs. wavelength(exp. Data)

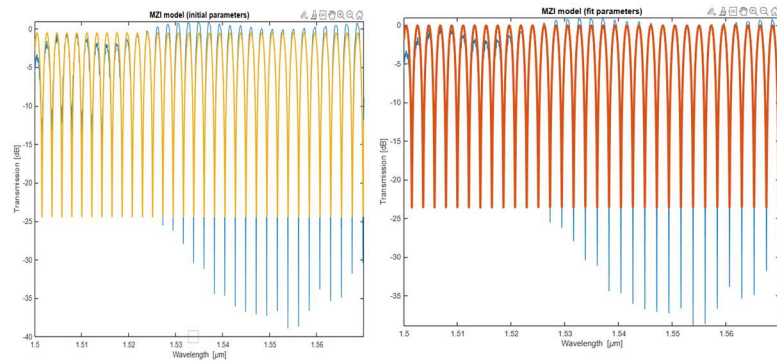


Figure 48.MZI model initial parameters

Figure 49.MZI fit parameters

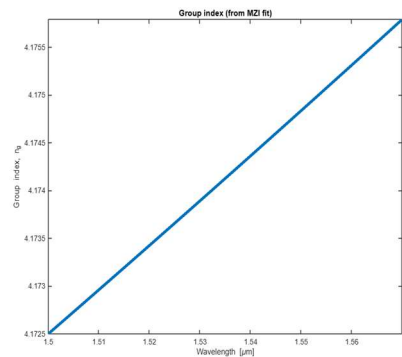


Figure 50. Group index vs. wavelength

2.2 Below is the summary of data collected using MATLAB for MZI2 Design which has a dL of 119.99um.

Below plots were done in MATLAB by correcting Baseline data and fitting the MZI spectrum with experimental data

MZI2 (dL = 119.99um)	Channel 1	Channel 2
FSR	4.725nm	4.725nm
Ng_av	4.1559	4.1559
x-fit	2.3879 -1.1936 -0.1072 0.0026 0.5374	2.3915 -1.1894 -0.1390 0.0046 1.1313
R^2	0.8997	0.9204
Ng0	4.2119	4.205
Waveguide parameters at wavelength	1.5282 um	1.5305
Dispersion	1092.7818 [ps/nm/km]	1419.4715

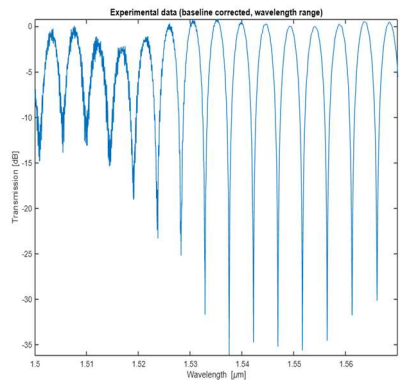


Figure 51. Baseline corrected exp. data

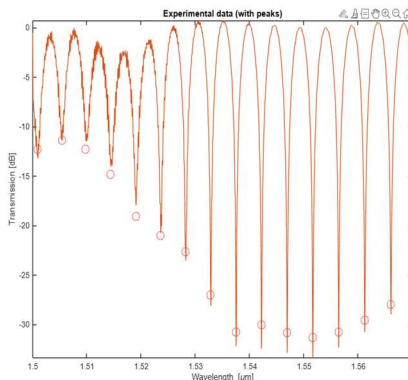


Figure 52. Exp. data with peaks

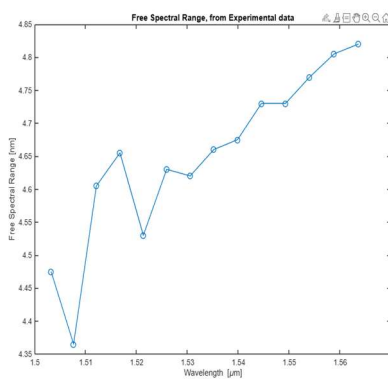


Figure 53. FSR from exp. data

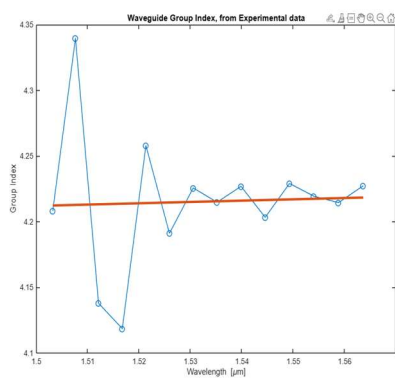


Figure 54. Group index vs. wavelength

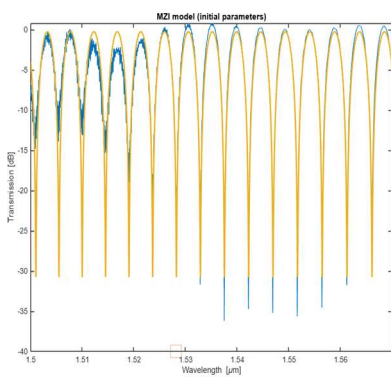


Figure 55. MZI model initial parameters

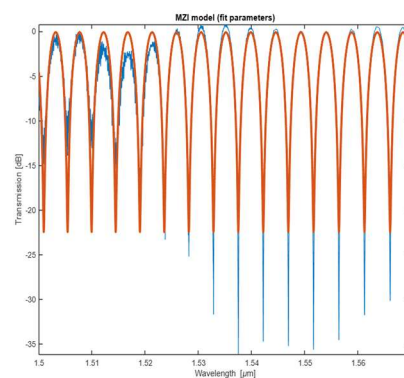


Figure 56. MZI fit parameters

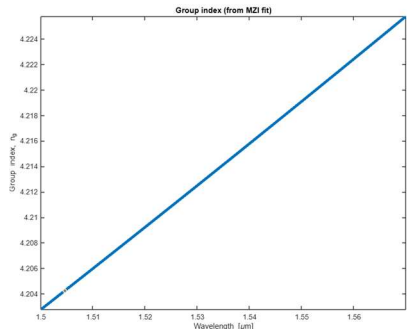


Figure 57. Group index vs. wavelength

2.3 Below is the summary of data collected using MATLAB for MZI3 Design which has a dL of 258.442um.

Below plots were done in MATLAB by correcting Baseline data and fitting the MZI spectrum with experimental data

MZI3 (dL = 258.442um)	Channel 1	Channel 2
FSR	2.2nm	2.175nm
Ng_av	4.1441	4.1917
x-fit	2.4113 -1.1564 -0.0068 0.0066 2.9947	2.3991 -1.1650 -0.0603 0.0077 3.4616
R^2	0.9092	0.8923
Ng0	4.1864	4.1851
Waveguide parameters at wavelength	1.5318um	1.5328um
Dispersion	67.9394 [ps/nm/km]	616.1632 [ps/nm/km]

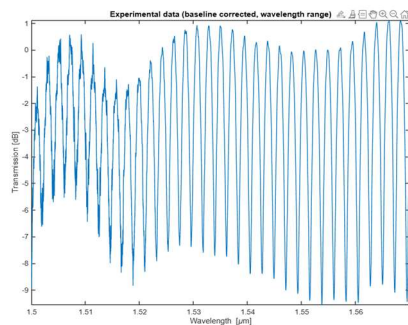


Figure 58. Baseline corrected exp. data

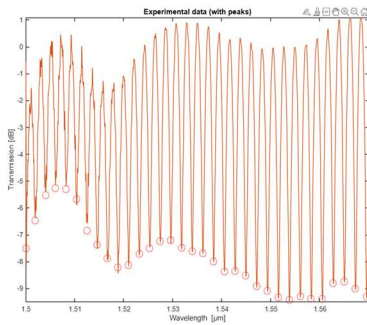


Figure 59. Exp. data with peaks

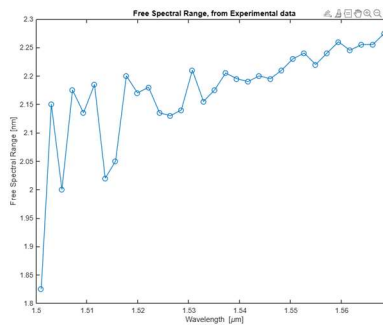


Figure 60. FSR from exp. data

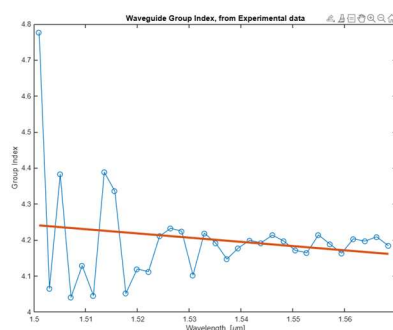


Figure 61. Group index vs. wavelength

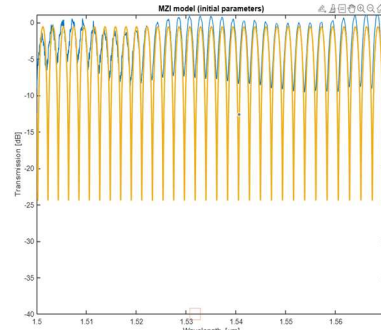


Figure 62. MZI model initial parameters

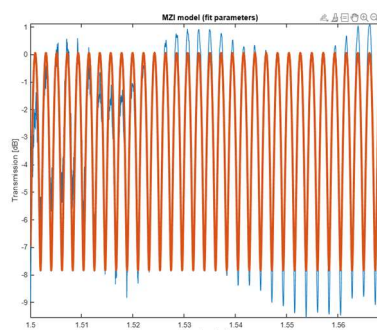


Figure 63. MZI fit parameters

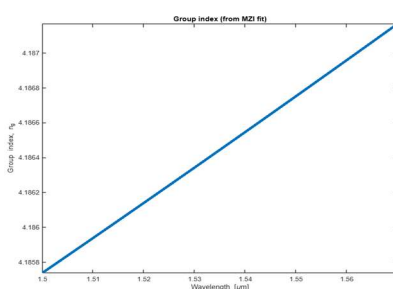


Figure 64. Group index vs. wavelength

2.4 Below is the summary of data collected using MATLAB for MZI4 Design which has a dL of 183.714um.

Below plots were done in MATLAB by correcting Baseline data and fitting the MZI spectrum with experimental data

MZI4 (dL = 183.714um)	Channel 1	Channel 2
FSR	3.1nm	3.11nm
Ng_av	4.1373	4.1240
x-fit	2.3965 -1.1738 -0.0173 0.0026 0.9119	2.3941 -1.1767 -0.0173 0.0028 0.9407
R^2	0.93941	0.9245
Ng0	4.1975	4.1943
Waveguide parameters at wavelength	1.5314	1.5299um
Dispersion	176.9615 [ps/nm/km]	176.5855 [ps/nm/km]

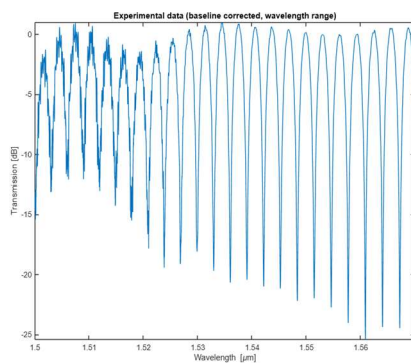


Figure 65. Baseline corrected exp. data

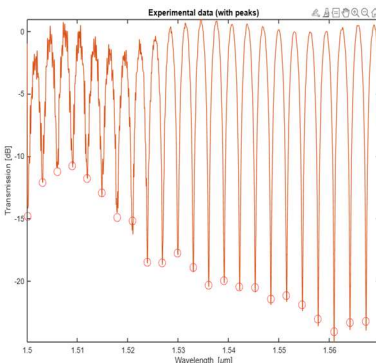


Figure 66. Exp. data with peaks

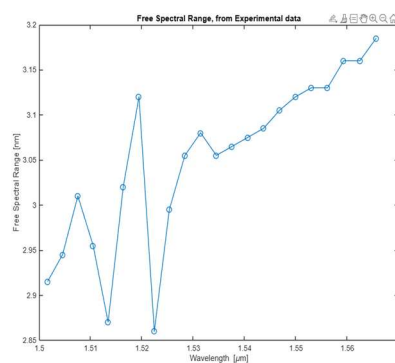


Figure 67. FSR from exp. data

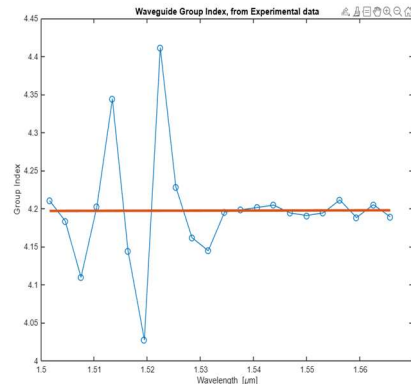


Figure 68. Group index vs. wavelength

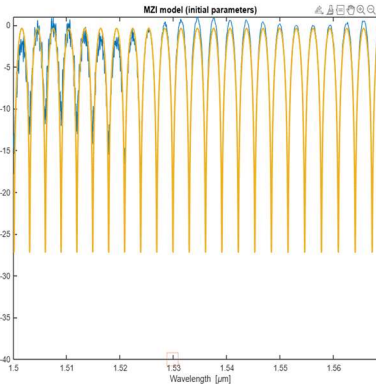


Figure 69. MZI model initial parameters

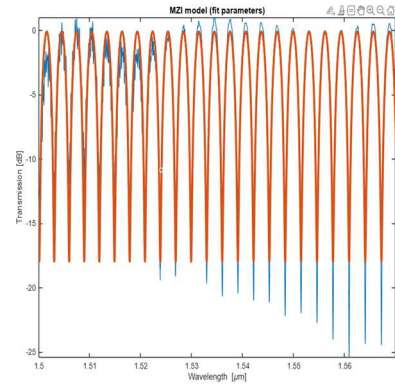


Figure 70. MZI fit parameters

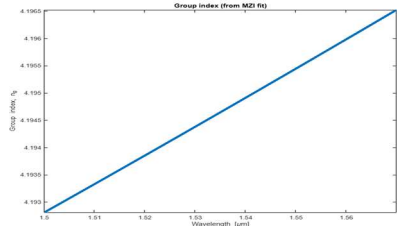


Figure 71. Group index vs. wavelength

IX. Conclusion

Based on the Corner Analysis using MODE and actual Measurement data obtained, here is the table summarizing the data.

From Section V

The max. group index obtained from Corner Analysis using MODE is = 4.256

The min. group index obtained from Corner Analysis using MODE is = 4.185

From Section VI

The mean FSR from Monte Carlo simulations for MZI1 Design is = 2.23 nm

The mean FSR from Monte Carlo simulations for MZI3 Design is = 2.20nm

From measurement data in section VIII, group index and FSR values align closely with corner analysis data. For MZI1 design, $ng = 4.17$ and $FSR = 2.24\text{nm}$. For MZI3 design, $ng = 4.18$ and $FSR = 2.2\text{nm}$.

Based on below table with delta L from my MZI Designs, we observe that group index decreases with increasing delta L.

DL (delta L) (um)	ng	FSR (nm)
183.714	4.19	3.11
258.442	4.18	2.2
119.99	4.21	4.72
256.332	4.17	2.24

Acknowledgments:

I acknowledge the edX UBCx Phot1x Silicon Photonics Design, Fabrication and Data Analysis course, which is supported by the Natural Sciences and Engineering Research Council of Canada (NSERC) Silicon Electronic-Photonic Integrated Circuits (SiEPIC) Program. The devices were fabricated by Richard Bojko at the University of Washington Washington Nanofabrication Facility, part of the National Science Foundation's National Nanotechnology Infrastructure Network (NNIN), and Cameron Horvath at Applied Nanotools, Inc. Omid Esmaeeli performed the measurements at The University of British Columbia. We acknowledge Lumerical Solutions, Inc., Mathworks, Mentor Graphics, Python, and KLayout for the design software.

References:

- [1] R. J. Bojko, J. Li, L. He, T. Baehr-Jones, M. Hochberg, and Y. Aida, "Electron beam lithography writing strategies for low loss, high confinement silicon optical waveguides," *J. Vacuum Sci. Technol. B* 29, 06F309 (2011)
- [2] Lukas Chrostowski, Michael Hochberg, chapter 12 in "Silicon Photonics Design: From Devices to Systems", Cambridge University Press, 2015
- [3] <http://siepic.ubc.ca/probestation>, using Python code developed by Michael Caverley.
- [4] Yun Wang, Xu Wang, Jonas Flueckiger, Han Yun, Wei Shi, Richard Bojko, Nicolas A. F. Jaeger, Lukas Chrostowski, "Focusing sub-wavelength grating couplers with low back reflections for rapid prototyping of silicon photonic circuits", *Optics Express* Vol. 22, Issue 17, pp. 20652-20662 (2014) doi: 10.1364/OE.22.020652
- [5] www.plcconnections.com, PLC Connections, Columbus OH, USA.
- [6] <http://mapleleafphotonics.com>, Maple Leaf Photonics, Seattle WA, USA.